UNIVERSITY OF CALIFORNIA, SAN DIEGO

ANALYSIS OF SPERMATOZOA MOTILITY AND DNA INTEGRITY FOLLOWING IRRADIATION WITH 633 NM LIGHT

A Thesis submitted in partial satisfaction of the requirements for the degree Master of Science

in

Bioengineering

by

Kay Wen Chow

Committee in Charge:

Professor Michael W. Berns, Chair
Professor Stephanie Fraley, Co-Chair
Professor Pedro Cabrales

2017

The thesis of Kay Wen Chow is approved, and it is acceptable in quality and form for publication on microfilm and electronically:

Co-Chair

Chair

University of California, San Diego

2017

Dedication

To my loving parents, May and Norman, who have supported me throughout my life and encouraged me to strive to be the best that I can be.

Table of Contents

List of Figures and Tables

List of Abbreviations

8-oxo-G: 8-hydroxyguanine

CASA: computer assisted sperm analysis

COM: center of mass

Cox: cytochrome c oxidase

HTF: human tubal fluid

LLLT: low-level light therapy

MSD: mean squared displacement

PSD: power spectral density

ROS: reactive oxygen species

SSS: serum substitute supplement

TBF: tail beat frequency

VCL: curvilinear velocity

Acknowledgements

I would like to acknowledge and thank all of those individuals who supported and guided me along my educational journey. Without them, I would not be the person that I am today.

I am grateful for Professor Michael W. Berns, who allowed me to be a part of his lab without having any prior research experience. Not only has he shared his wealth of knowledge with me, but he has cared for not only my success, but the success of every member of his lab.

I would like to thank Dr. Daryl Preece, without whose guidance and expertise the completion of this thesis would not be possible. He has dedicated countless hours of his time to training and coaching me grow as a researcher and as an individual. He exceeded expectations as a mentor and never hesitated to offer his advice on all facets of life.

I would like to thank Dr. Veronica Gomez-Godinez for all of her assistance with running assays and understanding cell biology, as well as for her never-ending kindness and patience. I would like to thank Linda Shi, for her assistance with troubleshooting when problems inevitably arose with equipment, and Michelle Duquette, for giving thoughtful suggestions for my experiments.

I would like to thank Aaron, Chris, Derrick, Justine, Matt, Shirli, and Vikash for working alongside me at odd hours of the day. Without their support and company, long hours in the lab would not have been as enjoyable. I wish them all the best of luck in the remainder of their studies and future endeavors.

Thanks to my family: my parents, May and Norman, and my siblings, June, Sharon, and Shawn, for all of their love and advice. Finally, I would like to thank all of the friends

I have made along the way and those that have stayed by my side. From study sessions, to (more importantly) study breaks, I could not have gotten through undergraduate and graduate school without them.

Chapter 2, in part, is a reprint of the material published as it appears in "Red light improves spermatozoa motility and does not induce oxidative DNA damage" by D. Preece, K.W. Chow, V. Gomez-Godinez, K. Gustafson, S. Esener, N. Ravida, B. Durrant, M.W. Berns. *Sci. Rep.* **7,** 46480 (2017). The thesis author was the second author of the paper, but contributed equal amount of effort as the first author.

Chapter 4, in part, is a reprint of the material published as it appears in "Effect of red light on optically trapped spermatozoa" by K.W. Chow, D. Preece, M.W. Berns. *Biomed. Opt. Express* **8,** 4200-4205 (2017). The thesis author was the first author of this material.

ABSTRACT OF THE THESIS

ANALYSIS OF SPERMATOZOA MOTILITY AND DNA INTEGRITY FOLLOWING IRRADIATION WITH 633 NM LIGHT

by

Kay Wen Chow

Master of Science in Bioengineering

University of California, San Diego 2017

Professor Michael W. Berns, Chair
Professor Stephanie Fraley, Co-Chair

Reproductive success is dependent on the ability of spermatozoa to reach and fertilize the oocyte. Although there are numerous assisted reproductive technologies that were developed for human use, not all are as effective in animals due to large variations in reproductive biology. The use of drugs and excessive handling on nondomestic animals may induce additional stress. Thus, there is a need for novel noninvasive, drug-free fertility

treatments that are applicable across a range of species. Sperm swimming speed and swimming force are two measures of sperm quality; improvement of these qualities may increase the chances of successful reproduction. It is believed that red light irradiation stimulates cytochrome c oxidase in the mitochondria to increase ATP production. However, stimulation of the electron transport chain has been shown to increase reactive oxygen species, which may have negative effects on sperm DNA. In this thesis, the efficacy of red light irradiation for improving sperm swimming speed and swimming force and its effect on DNA are assessed. Human spermatozoa were irradiated with a monochromatic, coherent 633 nm laser for 30 minutes. Swimming speed was measured using a wavelet-based tracking algorithm implemented in LabVIEW. Swimming force was measured using optical trapping and position tracking. Oxidative DNA damage was assessed using single-cell imaging following immunofluorescent staining for double-strand breaks and an enzyme-linked immunosorbent assay for oxidized guanine. Both sperm swimming speed and swimming force increased after irradiation without significant DNA damage.

Chapter 1: Introduction

1.1 Spermatozoa Physiology

Spermatozoa are the gamete cells responsible for carrying and delivering genetic information from the male to the female. Sperm cells consist of 3 main sections: the head, which contains tightly packed genomic DNA as well as the acrosome; the midpiece, packed with 50-75 coupled mitochondria; and the tail, a single flagellum that propels the sperm[1]. Dynein molecular motors, powered by ATP hydrolysis, are responsible for the characteristic flagellar beat that allows sperm to swim towards the egg. The rate at which this movement occurs is known as the tail beat frequency (TBF).

The acrosome reaction is triggered upon sperm-egg contact. The acrosome contains enzymes, such as hyaluronidase and acrosin, which digest the outer layers of the egg. These enzymes are released when the sperm makes contact with the egg. The egg cell is surrounded by the zona pellucida, a glycoprotein layer adherent to sperm. After one sperm cell penetrates and fuses with the ovum, the zona glycoproteins are modified so that other sperm cannot bind to or penetrate the zona[2]. In most mammalian species, the zona is surrounded by a layer of cells known as the cumulus oophorus that helps to protect the egg[3]. Sperm must be able to penetrate both of these layers to fertilize the egg.

Sperm are not fully capable of fertilizing the egg until they are activated, which requires hyperactivation and capacitation. Hyperactivation is a process, regulated by Ca^{2+} intake and reactive oxygen species (ROS) signaling, during which sperm reach full motility[4]. Upon entering the female reproductive tract, sperm calcium channels (CatSper) are activated and Ca^{2+} uptake is initialized; Ca^{2+} uptake is required for hyperactivation,

capactiation, and regulation of the acrosome reaction[5]. Ca^{2+} has been shown to increase sperm tail thrusting motions[6]. Thus, an increase in Ca^{2+} may lead to an increase in sperm swimming force.

1.2 Low-Level Laser Therapy

Low-level laser therapy (also known as low-power laser irradiation, low-level light therapy, and laser biostimulation) (LLLT) is the use of red or near-infrared light at low powers (1-500 mW) on cells and and tissue for therapeutic purposes. Unlike most other laser therapies, LLLT is based on a photochemical effect rather than ablation or the effects of heating[7]. Common applications include wound healing, cell proliferation, angiogenesis, and pain relief[8–11]. Application of red laser and LED to A549, U2OS, and PTK2 cell cultures resulted in increased cell migration following scratch tests[12]. Another study saw increased tissue regeneration and expression of angiogenic growth factors in human adipose-derived stem cell spheroids in mouse skin models following irradiation with 660 nm light[9]. The mechanism for these improvements is believed to be red light stimulation of Complex IV of the electron transport chain, also known as cytochrome c oxidase (Cox). Cox has been shown to be a photoacceptor for light in the wavelengths between 600-860 nm, similar to the absorption spectra for biological responses to light such as DNA and RNA synthesis[13]. It is possible that absorption of these wavelengths results in an increase in activity for the enzyme.

Cox is responsible for the generation of water molecules from protons, electrons, and oxygen molecules at the end of the electron transport chain. It also contributes to the formation of the proton gradient across the mitochondrial membrane, allowing ATP synthase to produce ATP. Passarella et al. observed an increase in ATP generation in

isolated rat liver mitochondria in response to 632.8 nm irradiation at 15 mW[14]. Wong-Riley et al. found that Cox activity increased in neurons in conjunction with increases in ATP content in response to irradiation from a 670 nm LED[15]. Pastore, Greco, and Passarella compared the effect of 632.8 nm light on isolated reduced cytochrome c and Cox and concluded that laser stimulation increases ATP generation in Cox, but not in cytochrome c, indicating preferential targeting of Cox[16]. Therefore, red light stimulation increases ATP generation in mitochondria, though the effects appear to be dose and duration dependent.

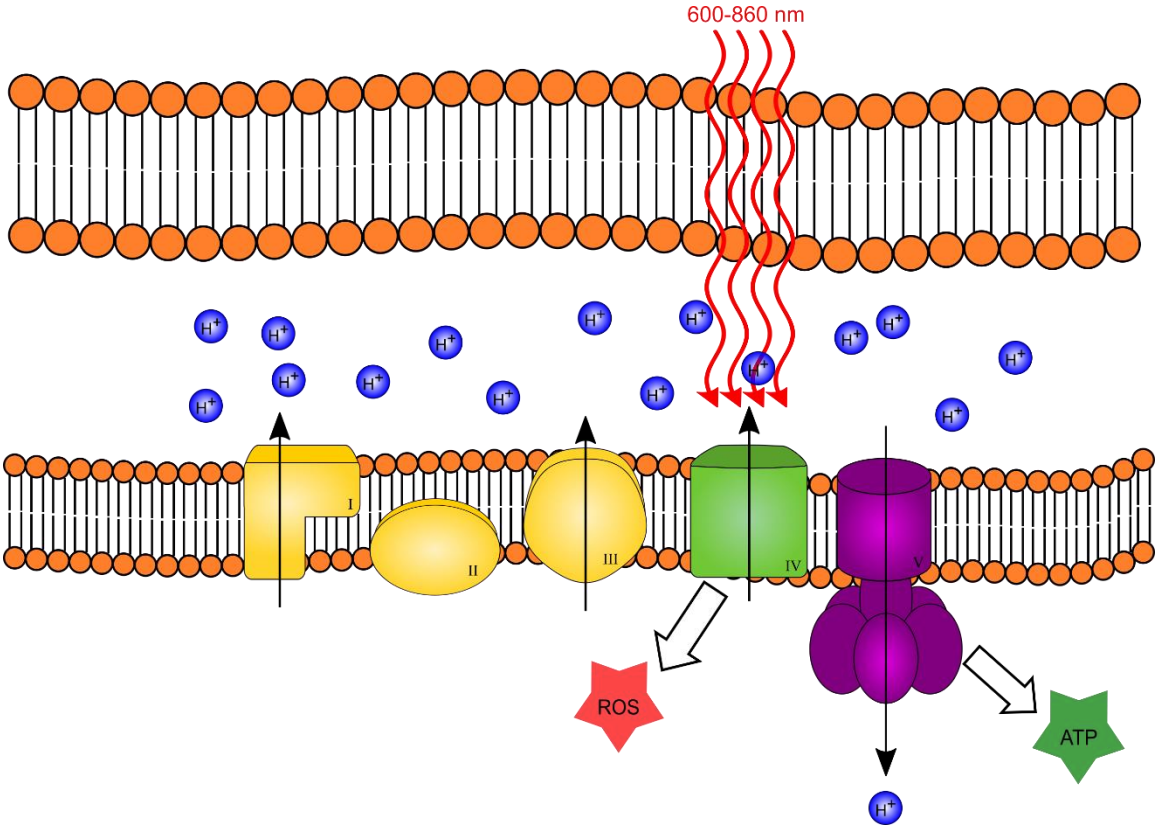

Figure 1.1. Red light stimulation of Cox in the electron transport chain. Black arrows show flow of protons across the inner mitochondrial membrane.

In addition to the generation of ATP, the electron transport chain produces ROS, such as superoxide anion (O_2^-) and hydrogen peroxide (H_2O_2), as a byproduct of the formation of water molecules. LLLT has been shown to increase ROS production in low

levels that may be important for the activation of transcription factors, some of which upregulate genes related to proliferation, migration, and production of growth factors[7,17]. Normally, excess ROS are scavenged by endogenous antioxidants, but large excesses of ROS can lead to oxidative stress. Oxidative stress can cause oxidative DNA damage that can lead to genetic abnormalities and mitochondrial damage that may induce apoptosis.

LLLT has been shown to increase the release of the free radical nitric oxide (NO). NO acts as a vasodilator which may help relieve pain by increasing blood flow[18]. It is believed that NO inhibits cytochrome c oxidase through competitive binding with O_2. The observed increase in NO following LLLT is believed to be partially due to photodissection of NO from cytochrome c oxidase, both decreasing inhibition of Cox and increasing the availability of NO for endogenous and exogenous use[7]. Cox also contributes to the generation of NO through the reduction of NO_2^-. It was shown that irradiation with 590 nm light led to an increase in NO production via this pathway[19].

Because spermatozoa are dependent on ATP for motility, LLLT can be beneficial for sperm function. Successful triggering of the acrosome reaction and delivery of genetic information is dependent on its ability to swim to the oocyte. The sperm flagellum is powered by dynein molecular motors, which rely on the hydrolysis of ATP to create the characteristic power stroke. In theory, an increase in ATP supply will allow the sperm tail to beat at a faster rate, limited by the maximum rate of ATP consumption. LLLT has also been associated with increases in Ca^{2+} transport in sperm[20,21], which may lead to an increase in the thrust of the sperm tail. The increased production of ROS and NO may aid in sperm activation through their roles as secondary messengers[4]. However, due to the high density of mitochondria and limited access to antioxidants, sperm may be prone to

oxidative stress[22]. It is therefore imperative to carefully analyze the effect of LLLT on sperm DNA integrity.

1.3 Optical Trapping

Since the invention of the single-beam gradient trap by Ashkin in 1986[23], optical tweezers have been applied to single cells as well as smaller structures such as single strands of DNA. In optical trapping, a near infrared laser beam is focused through an objective lens of high numerical aperture to produce a steep intensity gradient. Near-infrared wavelengths are typically used in biological applications to minimize damage to cells, since most biological structures absorb weakly at these wavelengths. For particles larger than the wavelength of light, optical trapping can be described by ray optics[24]. As rays of light travel through a particle, they are refracted, causing a change in their momentum. Due to Newton's third law, an equal and opposite momentum must then be imparted to the particle. This change in momentum gives rise to the optical restoring force used to confine particles. The optical force is proportional to the gradient of the intensity of light. Particles with refractive index higher than the surrounding medium experience a force in the direction of the positive optical gradient while particles with refractive index lower than the medium experience a force in the opposite direction[24].

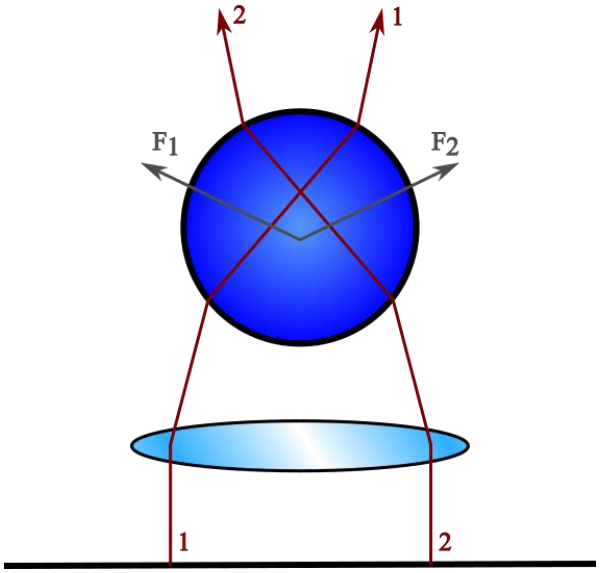

Figure 1.2. Ray optics description of optical trapping. Red lines indicate the propagation of laser light through the lens and particle. Gray lines, denoted as F_1 and F_2, indicate the resulting optical forces. There is a net force on the particle in the axial direction towards the laser focus.

Piconewtons of force can be applied to move and manipulate the trapped particle. Some biological applications include characterization of the forces exerted by molecular motors[25], chromosome separation during mitosis[26], and measuring swimming forces of spermatozoa[27]. The forces exerted by cells and biological molecules are often measured by conjugating a spherical bead to the structure to be measured, trapping the bead, pulling the bead with tweezers, and measuring its position in the trap. This method is especially useful when the particle of interest is too small to be trapped directly, such as DNA and proteins. By using a bead with known mechanical properties as a handle, the biomechanics of cellular structures, such as membranes and proteins, can be characterized.

Optical forces are rarely measured directly, but rather rely on the Hookean relationship with trap stiffness. Trap stiffness can be calculated from the corner frequency of the power spectrum, f_0, of a trapped spherical particle by the following relationship[28]

$$f_0 = \frac{\kappa}{2\pi\gamma} \tag{1.1}$$

where κ is the trap stiffness and γ is the drag force. Spherical objects of known radius are typically used to calibrate trap stiffness because of the homogeneity of their refractive indices and ease of calculating drag force. Due to the difficulty of determining drag forces of inhomogeneous objects, such as cells, this calibration method may not be optimal for living systems. An alternate method of determining trap stiffness is through equipartition theory, based on thermal fluctuation of Brownian particles.

$$\kappa = \frac{k_b T}{< x^2 >} \tag{1.2}$$

where k_b is the Boltzmann constant, T is the temperature, and $<x^2>$ is the variance in position of the trapped particle.

Sperm swimming force can be used to describe sperm quality, as it is directly related to the sperm's ability to penetrate the zona pellucida and cumulus oophorus of the egg. In this thesis, optical trapping is used to determine relative sperm swimming forces and tail beat frequency with and without LLLT.

Chapter 2: The Effect of Red Light Irradiation on Spermatozoa DNA

2.1 Introduction

Current methods of assisted reproduction for humans and animals rely on the use of drug and hormone intervention to improve success rates. Because many animals do not respond predictably to treatment designed for human use, there is heavier reliance on the use of high quality spermatozoa for reproduction. Spermatozoan quality can be described as its ability to successfully reach and fertilize the egg. One metric of sperm quality is its motility, which is commonly measured using the computer-assisted sperm analysis (CASA) system. The CASA system determines motility parameters by capturing a series of images at a tunable frame rate (e.g. 60 Hz) and tracking the trajectory of the centroid of each sperm[29]. CASA systems use high-powered flash lamps to record images. CASA systems track sperm based on the brightest pixel value. Under coherent light, sperm appear dark over a light background, affecting CASA motility measurements. Thus, a novel wavelet tracking algorithm to measure VCL under both coherent and incoherent illumination has been developed. This allowed for the direct comparison of sperm VCL under red light irradiation and brightfield illumination.

Red light irradiation of spermatozoa has been shown to increase sperm swimming speed and overall fertilizing potential[20,30–34]. One study showed an increase in oligospermic (low sperm count) and asthenospermic (low sperm motility) human sperm VCL in response to 905 nm laser light[31]. Another study saw an increase in fresh boar sperm VCL and mitochondrial membrane potential following treatment with red LEDs[32]. Sperm viability

following irradiation was characterized by testing membrane integrity with propidium iodide.

Although many studies have characterized the effect of red light irradiation on VCL, few have analyzed its effect on DNA integrity. It has been shown that 630 nm laser light stimulation can lead to the production of reactive oxygen species (ROS) in the mitochondria of mouse sperm[33]. Although low levels of ROS play an important role as messengers, such as allowing for capacitation of the sperm acrosome[4], high levels of ROS can be damaging to cell DNA. Previous studies have shown that oxidative stress from ROS is a major cause of DNA fragmentation in sperm[35]. DNA damage in sperm has been linked to male infertility, miscarriage, and high morbidity rates of offspring[36]. Therefore it is important to assess the effect of red light irradiation on DNA integrity.

Two methods of testing for oxidative DNA damage are assessing the quantities of (1) γH2AX and (2) 8-hydroxyguanine (8-oxo-G). A previous study showed that sperm are capable of phosphorylating histone H2AX on Serine 139 in the presence of H_2O_2[37]. This protein modification is termed γH2AX and is used by the cell to mark double-strand breaks up to 1-2 megabases beyond the damage site. Therefore it is deemed to be a highly sensitive marker for DNA double-strand breaks produced by ROS[38,39]. Similarly, 8-oxo-G can be formed in response to oxidative stress. ROS can damage DNA, causing oxidation of guanine in the DNA that is correlated with DNA fragmentation and strand breaks[40]. If left unrepaired, the oxidized guanine may pair with adenine instead of cytosine, resulting in mutations in DNA.

Many studies on the effect of red light irradiation on sperm consider its effect on membrane integrity[41–48], but few analyze the potential generation of oxidative DNA

damage. Because the proposed method in this study is intended for fertilization and live birth, testing the effect of 633 nm irradiation on sperm DNA is critical. By monitoring γH2AX formation, the localization of DNA double strand breaks can be observed. Immunofluorescent staining for γH2AX allows for the quantification of fluorescence intensity to determine overall severity of damage as well as identification of γH2AX foci, which show localization of double-strand breaks in the nuclear DNA. The concentrations of 8-oxo-G were measured following red light irradiation using a quantitative enzyme linked immunosorbent assay (ELISA) to determine whether irradiation led to significant levels of oxidative DNA damage.

2.2 Materials and Methods

2.2.1 Sample preparation

Cryogenically frozen human sperm samples were obtained from Infertility, Gynecology, and Obstetrics Medical Group (San Diego, CA). Samples were collected from healthy men and frozen according to a standard human freezing protocol[49,50]. The samples were thawed in a water bath at 37°C and centrifuged for 10 minutes at 208 g and the pellet was resuspended in 1 mL modified human tubal fluid (HTF) (Irvine Scientific, Irvine, CA) with 5% serum substitute supplement (SSS) (Irvine Scientific, Irvine, CA). The samples were washed once more in this media and resuspended for a final concentration of 30000 sperm/mL.

2.2.2 Red light stimulation

To assess the effect of red light irradiation on sperm motility, live sperm were irradiated for 35 minutes from above using a monochromatic, coherent 633 nm laser (Intense 7404, North Brunswick, NJ) at an intensity of 5.66 mW/cm^2 coupled to a

multimode fiber with beam homogenizer (Medlight FD, Switzerland) to ensure uniform exposure. To assess the effect of red light irradiation on sperm DNA, sperm were irradiated for 30 minutes from above using the same light source at an intensity of 31 mW/cm^2. Temperature change in the sample as a result of irradiation was assessed by periodically measuring the temperature of the dish with an infrared thermometer (Raytek Raynger MX2, Santa Cruz, CA). No significant change in temperature was recorded over the duration of the experiments.

2.2.3 Analysis of motility

In order to measure sperm swimming speed while under the influence of red light, a wavelet-based tracking algorithm implemented in LabVIEW was used to measure VCL. Wavelet analysis is used to determine what particles are most likely to be sperm. The algorithm sorts through a stack of images based on frequency to differentiate motile sperm (high frequency information) from non-motile sperm (low frequency information). The identified sperm can then be tracked using a modified Kalman filter, which determines the VCL of each sperm by predicting their trajectories and comparing the predictions with their current positions.

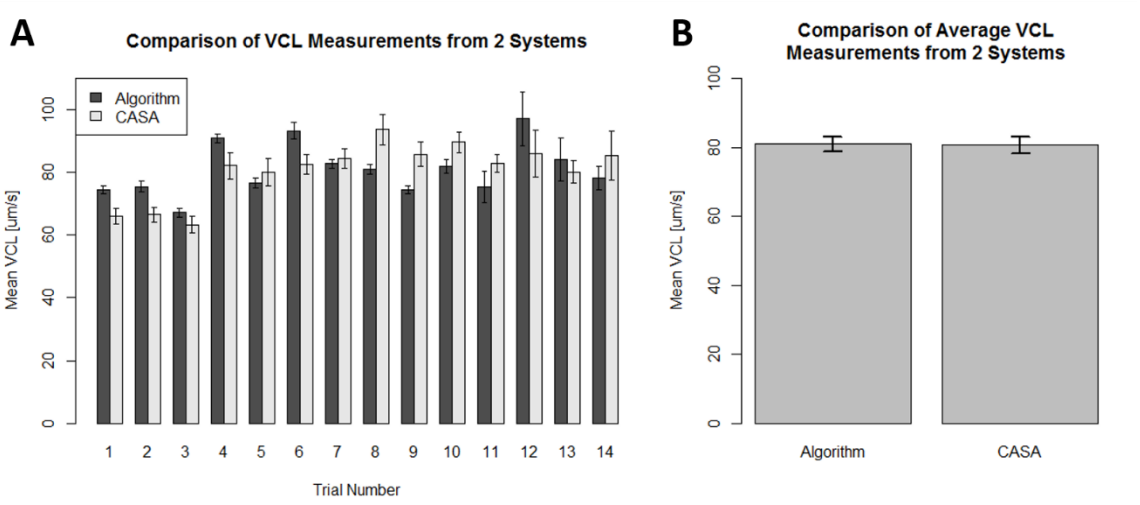

Figure 2.1. Comparison of VCL measurements from CASA and wavelet-based algorithm. Error bars in both graphs indicate standard error. (A) Mean VCL Measurements from 14 Trials. VCL measurements from the algorithm are multiplied by the scaling factor (1.59)

The results of the algorithm were compared with those from the IVOS CASA system (Hamilton Thorne, Baltimore MD). Two 6 μL aliquots of sperm were drawn from the same sample and VCL was measured using both systems simultaneously. This experiment was repeated for 14 trials. It was concluded that the measurements made from the two systems differed by a factor of 1.59 ± 0.17 μm/s. However, after adjusting for the scaling factor, there was no statistically significant difference between the VCL measurements made from the two systems (Figure 2.1). This indicates that the wavelet-based tracking algorithm is consistent with the CASA system, the gold standard in the fertility industry. Subsequent VCL measurements were taken using the wavelet-based tracking algorithm. 5 trials were conducted, with each trial representing the averaged VCLs of 4 aliquots taken from a single specimen imaged 1–2 minutes apart. Within each trial, approximately 1000 individual sperm traces were measured per test group. Samples from 2 different donors were used.

2.2.4 Imaging

Live sperm were imaged using a 40x NA 1.3 phase III oil immersion objective (Zeiss) on a Zeiss Axiovert S100 2TV microscope with a CMOS camera (Cohu 7800, San Diego, CA). A diagram of the imaging set up is shown in Figure 2.2. DNA damage was assessed via fluorescent imaging using a 63x NA 1.4 phase III oil immersion objective on a Zeiss Axiovert S100 2TV microscope with a CMOS camera (Hamamatsu ORCA-flash 4.0, San Diego, CA).

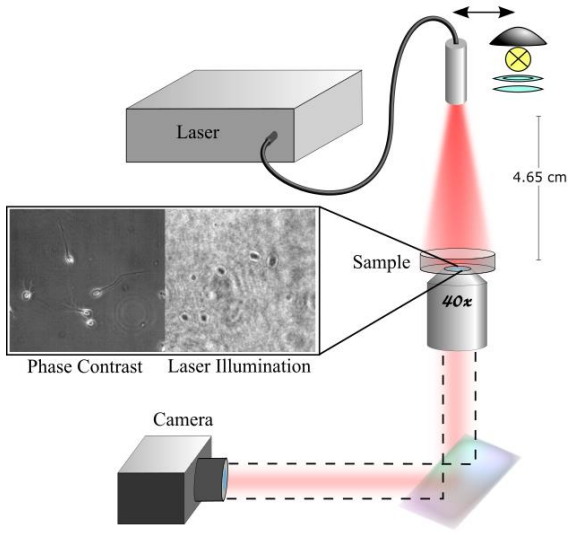

Figure 2.2. Optical setup for red light irradiation.

2.2.5 DNA damage detection

To test for DNA damage, a positive control was prepared by exposing live sperm to 1 mM H_2O_2 (Sigma, St. Louis, MO) in modified HTF for 2 hours. Three 50 µL sperm samples (1 positive control, 1 exposed to laser light, and 1 untreated sample) were plated on poly-d-lysine dishes (MatTek, Ashland, ME) to adhere them for imaging. The samples were fixed with 4% paraformaldehyde in phosphate buffered saline (PBS) for 1 hour and permeabilized with 500 µL blocking buffer for 1 hour. Blocking buffer was prepared with

5% horse serum and 0.2% Triton-X in PBS. The samples were stained with 1:1000 mouse anti-γH2AX antibody (Millipore, Billerica, MA) in blocking buffer for 1 hour. The samples were stained with 1:2000 anti-mouse secondary antibody in blocking buffer for 1 hour. The samples were stained with 1:600 DAPI (Invitrogen, Carlsbad, CA) in PBS for 10 minutes before imaging. The mean pixel intensity of γH2AX and γH2AX foci formation in the sperm head was assessed using ImageJ software (version 1.50a). A total of 297 sperm were imaged.

Oxidative DNA damage was further quantified using an 8-OHdG ELISA following the manufacturer's protocol (Cayman Chemical, Ann Arbor, MI). Samples of irradiated and untreated sperm were compared. Genomic DNA was extracted from 9 different sperm samples using a DNA isolation kit following the manufacturer's protocol (Zymo, Irvine, CA). Sperm DNA was assayed at a concentration of $1.5x10^7$ pg/mL in triplicate. Concentrations of damaged DNA were calculated using a standard curve prepared by assaying 8 samples of known 8-oxo-G concentration (between 10.3 pg/mL and 3000 pg/mL) in duplicate.

2.2.6 Statistical analysis

A post-hoc power analysis conducted in GPower 3.1.9.2 shows that a 3-group sample with n = 297 is sufficient to produce an effect size of 0.25 and α error probability of 0.05 with a power of 0.977. Statistical significance was determined using $\alpha = 0.05$, where $p < 0.05$ indicates a less than 5% chance the test groups originated from the same population. A Shapiro-Wilk test indicated that the data used in this study were not normally distributed ($p < 0.05$). Thus, significance tests for non-normally distributed data were used. A Kruskal-Wallis one-way analysis of variance was used to determine whether there was

a significant difference in γH2AX intensities and whether there was a significant difference in γH2AX foci formation. A Welch's t-test was used to determine 8-oxo-G concentration between the experimental and negative control groups. Statistical analysis was done using R software (version 3.2.0).

2.3 Results

2.3.1 Swim velocity following red light stimulation

A Student's t-test showed that all samples irradiated with red laser light exhibited a statistically significantly higher average VCL than their control counterparts (Figure 2.3). Increases in swimming speed were observed 35 minutes after irradiation. A 17-47% increase in VCL was observed.

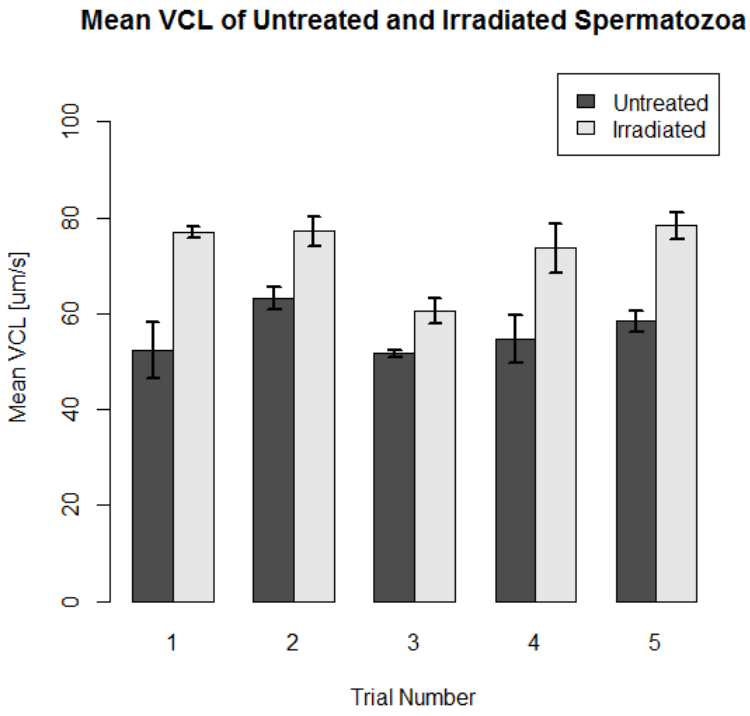

Figure 2.3. Comparison of mean VCL of spermatozoa before and after irradiation. Error bars indicate standard error.

2.3.2 Assessment of DNA damage following red light stimulation

Fluorescent images show localization of γH2AX in each of the test groups (Figure 2.4). Blue represents DAPI staining indicating the presence of nuclear DNA concentrated in the sperm head. Red represents γH2AX staining indicating the presence of double-strand DNA breaks. Overlaps in red and blue staining are representative of double-strand break formation in genomic DNA. The average fluorescence intensity and number of γH2AX foci across the sperm heads were quantified to determine the relative amounts of γH2AX formation (Figure 2.5). A total of 82 positive control sperm, 127 laser irradiated sperm, and 88 negative control sperm were analyzed. A Kruskal-Wallis test determined that there was no statistical significance between the mean pixel intensities of the experimental and negative control groups ($p = 0.6605$). The mean pixel intensity of the positive control group was determined to be significantly higher than that of the experimental and negative control groups ($p = 2.144 \times 10^{-10}$). The mean pixel intensities for the positive, experimental, and negative groups were 177.4, 93.5, and 91.9, respectively. A Kruskal-Wallis test indicated that the positive control had much larger numbers of γH2AX foci than the other two groups ($p = 1.474 \times 10^{-10}$). The numbers of γH2AX foci in the heads of sperm in the experimental group and negative control group were compared using a Kruskal-Wallis test ($p = 0.723$). The average number of γH2AX foci in the positive, experimental, and negative groups were 6.4, 2.6 and 2.6, respectively.

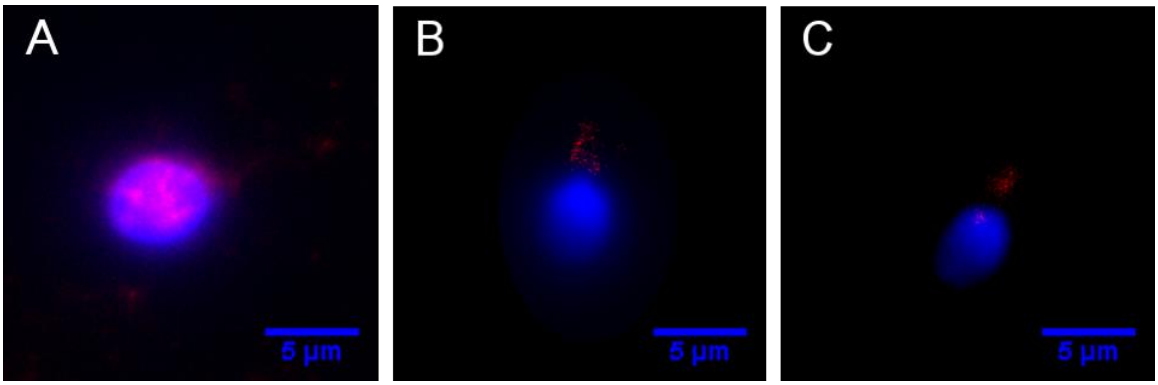

Figure 2.4. Fluorescent images of sperm stained with DAPI DNA dye and anti-γH2AX antibody. (A) Positive control. Sperm were treated with H_2O_2. (B) Experimental group. Sperm were exposed to 633 nm light for 30 minutes. (C) Negative control. Sperm were left untreated.

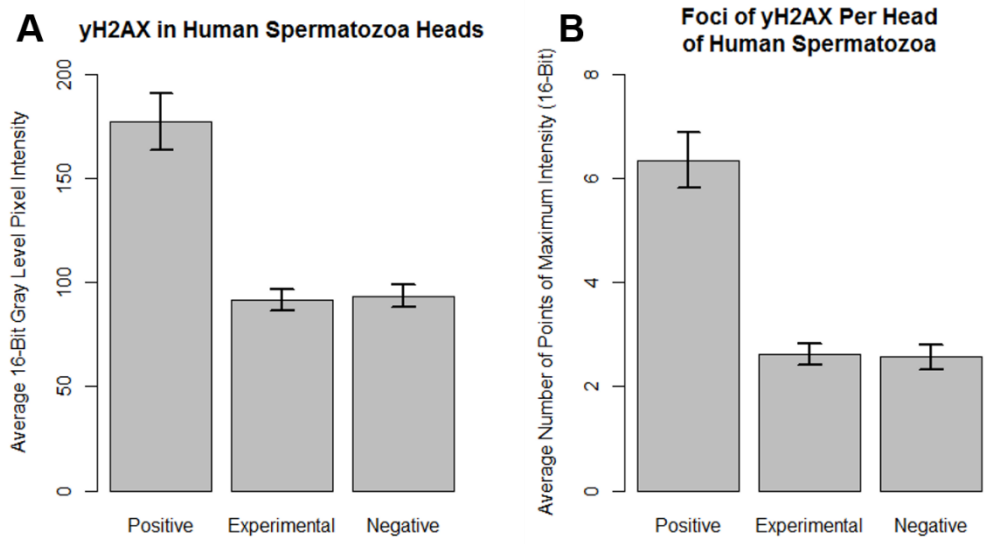

Figure 2.5. Quantification of double-strand DNA breaks in sperm using γH2AX. Error bars indicate standard error. (A) The mean pixel intensities for the positive, experimental, and negative groups were 177.4, 93.5, and 91.9, respectively. (B) The average number of γ H2AX foci in the positive, experimental, and negative groups were 6.4, 2.6 and 2.6, respectively.

A quantitative 8-OHdG ELISA was used to test for oxidative DNA damage. 9 independent sperm samples were tested for the presence of oxidative DNA damage at a concentration of 15 ng/μL. The percentages of DNA damage relative to the total DNA concentration are given in Figure 2.6. The difference in calculated concentrations of damaged DNA between the two test groups in each sample was not significantly significant ($p > 0.05$), in all but 1 sample, as determined by a Welch's t-test. In the sample where 8-oxo-G concentrations differed significantly (Sample 4 in Figure 2.6 below, $p = 0.000321$), the percentage of oxidative damage in the control and irradiated sample were 0.000311% and 0.000198%, respectively. Although oxidative damage was present in the samples, it makes up a small amount of the total DNA assayed. The percentage of oxidative DNA damage in both groups was 0.0003%.

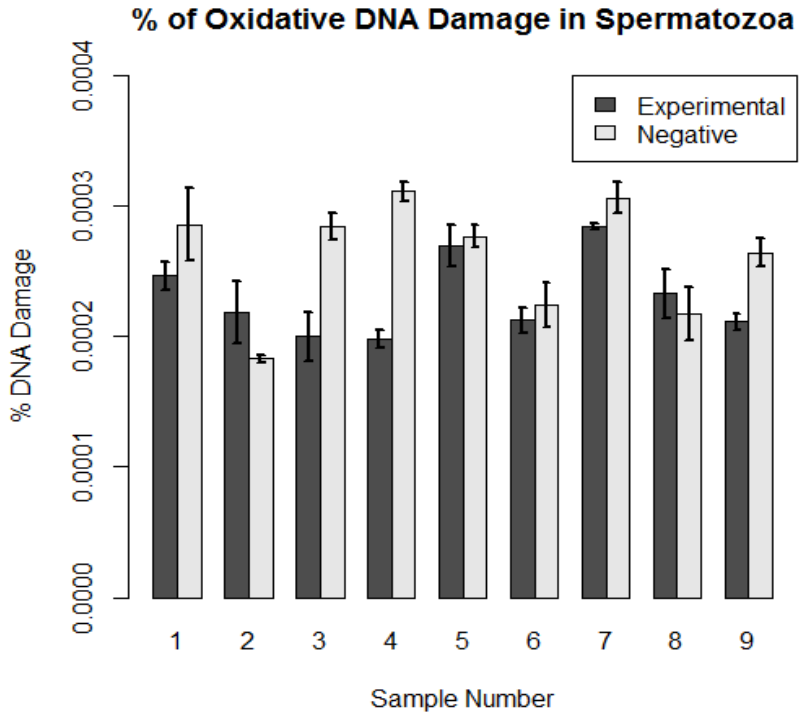

Figure 2.6. Quantification of oxidative DNA damage using 8-oxo-G ELISA. Error bars indicate standard error.

2.4 Discussion

This study indicates that 633 nm laser irradiation of sperm at a power density of 5.66 mW/cm^2 increases sperm swimming speed. This data supports the proposed chemical mechanism of intracellular photonic absorption, indicating that the photonic energy in red light is absorbed by Cox, increasing ATP production, and thus increasing sperm motility. In previous studies, the absorption spectra obtained for Cox in different oxidation states were recorded and found to be very similar to the action spectra for biological responses to light[13]. Therefore it was proposed that Cox is the primary photoacceptor for the red to NIR range in mammalian cells[13,51]. Photonic absorption in mitochondrial Cox boosts ATP production and energy supply and may increase mitochondrial Ca^{2+} uptake. In sperm, it is believed that this results in increased motility and increased fertilization potential[21]. It is possible that the observed increase in motility was due to local heating, rather than photochemical effects. However, assuming the absorption coefficient of water at 633 nm is 0.0029183 cm^{-1} the temperature rise due to laser illumination should be less than $2x10^{-4}$ degrees, which is not sufficient to affect motility.

Tracking micron-sized objects under coherent illumination is a difficult task. Due to the constantly moving fringes produced over the entirety of the image, algorithms that rely on shape or intensity information often fail. The wavelet-based approach that has been developed is a useful option especially under coherent illumination. The algorithm has some drawbacks, such as increased complexity and tendency to fail for completely dead sperm. However, for most cases it is remarkably robust and is certainly comparable to the conventional CASA systems which are relatively costly. In addition, the algorithm described here allows for the tracking of sperm during laser irradiation allowing the

observation of the direct effects of irradiation on swimming speed. This capability eliminates the lag period during which sperm are removed from the illumination source.

To be a viable fertility treatment, it is necessary that laser irradiation does not induce DNA damage in sperm. While past studies confirm that red light increases fertilizing potential, its effect on DNA integrity has not been fully assessed. Table 2.1 below indicates past studies of the effect of red light on spermatozoa quality and outlines the irradiation wavelength used, the species of the sperm analyzed, and the assay used to test sperm quality. While many studies assessed whether spermatozoa were still viable following irradiation, few looked specifically at its effect on DNA integrity.

Table 2.1. Prior work on irradiation of spermatozoa with visible and IR light. Sperm quality analysis tests listed above reflect tests of physical defects in sperm DNA and plasma membranes. Cell viability assays and hypo-osmotic swelling tests assess membrane integrity. Aniline blue staining assesses sperm chromatin condensation through the detection of lysine residues on sperm DNA[52]. The sperm chromatin dispersion test is used to measure DNA fragmentation based on chromatin morphology[53]. The sperm chromatin structure assay (described below) measures DNA fragmentation based on susceptibility to denaturation[54].

Sperm Quality Analysis	Species Tested	Irradiation Wavelength
cell viability assay (membrane integrity)	†bull[41,42]; †chicken[43]; †pheasant[43]; †turkey[43]; †ram[44]; *boar[32]; *turkey[43]; *rabbit[45]; *bull[46]	600-700 nm
	*human[55,56]	700-1064 nm
hypo-osmotic swelling test	†chicken[43]; †pheasant[43]; †turkey[43]; *human[47]; *dog[48]	600-700 nm
	*human[5]	800-1064 nm
ROS production	*ram[57]; *tilapia[57]; *human[34]	400-800 nm
	†bull[42]; *ram[57]; *tilapia[57]	600-700 nm
sperm chromatin structure assay	*human[31]	905 nm
aniline blue staining	*human[47]	636.6 nm
sperm chromatin dispersion	*human[5]	830 nm
none	*buffalo[58]	532 nm
	†bull[21,59]; †human[60]; *human[60–62]; *mouse[20,33]; *dog[63]	600-700 nm
	†bull[20,59]; *human[61,64]	700-1064 nm

†frozen specimens; *fresh specimens

DNA damage in spermatozoa has been associated with impaired fertilization, as well as with developmental problems and difficulties with embryonic implantation. Additional problems linked to DNA damage in sperm include miscarriage and high morbidity rates of offspring[36]. A cell's inability to cope with ROS has been linked to both DNA damage and a reduction in sperm motility[22]. The mitochondria are largely responsible for producing ROS within sperm cells and are thus likely to be responsible for causing oxidative stress. This study demonstrates that sperm exposure to 633 nm laser light at a power density of 31 mW/cm^2 does not cause significant levels of double-strand DNA

breaks, marked by γH2AX, nor did it induce significant levels of oxidative DNA damage, measured with 8-oxo-G. H_2O_2 causes the indirect formation of γH2AX, which can be detected 1-2 megabases from the break site[38]. The ability of this marker to spread would allow for easier detection of DNA damage than the more widely used sperm chromatin structure assay (SCSA), which measures DNA fragmentation. SCSA assesses DNA integrity using heat-induced or acid-induced denaturation. Damaged DNA is more susceptible to denaturation at high temperatures and at low pH conditions than intact DNA[54]. However, the source of DNA damage cannot be identified with this method. Testing for γH2AX is a highly sensitive method for detecting DNA damage caused by the production of ROS and oxidative stress in sperm. High levels of γH2AX in the sperm head were observed when exposed to H_2O_2, but little or no γH2AX in the laser-irradiated or negative control groups were detected. Some antibody binding is present in the sperm midpiece, where the mitochondria are concentrated. However, the mitochondrial DNA lack the H2AX histone. Therefore, it is likely that this is an effect of non-specific antibody binding, rather than an indication of the presence of double-strand breaks.

From the quantitative ELISA, it is evident that DNA damage was detected in the experimental and negative control groups. Similar levels were detected between the two, indicating that this is likely an artifact of centrifugation, cryopreservation, and thawing. There is some variation in the amount of damaged DNA present between samples. This is the result of variation in the quality of sperm from sample to sample (each sample was taken from a different ejaculate). In all cases, the amount of DNA damage detected was miniscule compared to the amount of DNA assayed. From this data, it is likely that laser irradiation did not result in high enough levels of ROS production to cause significant DNA

damage. By immunostaining with γH2AX and assaying for 8-oxo-G, it was determined that red light irradiation does not produce significant levels of oxidative damage in sperm nuclear DNA.

In order to further determine the safety of red light irradiation as a sperm motility treatment, additional DNA damage tests must be conducted. An ROS probe can be used to detect the production of ROS in the mitochondria as a result of laser irradiation. Tracking ROS may give insight into DNA repair pathways in sperm as well as ROS-induced DNA damage. Sperm DNA fragmentation assays, such as acridine orange, should be repeated in order to compare these results with those from previous studies[31]. Additionally, the proposed methodology and DNA damage analysis should be tested on fresh samples from men with poor sperm quality as well as on different animal species. Since sperm morphology and energetics are significantly different between species, the effect of photo-stimulation could also vary significantly between species. These results open up the possibility that red light exposure could be used to improve IVF results in humans and possibly in animals obviating the need for drug induced stimulation of sperm. The current technique could also be used in conjunction with established IVF techniques to improve treatment outcomes.

Acknowledgements

This material is based upon work supported by the Air Force Office of Scientific Research under award number FA9550-17-1-0193 and the National Heart, Lung and Blood Institute (NHLBI) of the National Institutes of Health under award number (RO1HL12136-02S1). Thank you to The San Diego Zoo Institute for Conservation Research, The Institute for Engineering in Medicine at UC San Diego, and The Beckman Laser Institute at UC

Irvine. The content of this paper is solely the responsibility of the authors and does not necessarily represent the official views of the National Institutes of Health and the United States Air Force.

Chapter 2, in part, is a reprint of the material published as it appears in " Red light improves spermatozoa motility and does not induce oxidative DNA damage" by D. Preece, K.W. Chow, V. Gomez-Godinez, K. Gustafson, S. Esener, N. Ravida, B. Durrant, M.W. Berns. *Sci. Rep.* **7,** 46480 (2017). The thesis author was the second author of the paper, but contributed equal amount of effort as the first author.

Chapter 3: A Device to Increase the Motility of Spermatozoa

3.1 Introduction

The conservation of endangered species relies on the development of novel assisted reproductive technologies. Although there are many techniques designed for human use, not all of them are successful in animals because many species have complex reproductive biology[65]. For example, in vitro fertilization (IVF) has had limited success due to complications with obtaining oocytes from the mother and implanting embryos fertilized in vitro[66]. Excessive animal handling and drug administration may induce additional stress in the animal. Therefore, there is a need for noninvasive reproductive techniques that are effective for a variety of species. Artificial insemination (AI) is among the least invasive, most universally applicable assisted reproductive technologies, but its success relies on the use of high quality spermatozoa[67]. One metric for evaluating sperm quality is swimming speed[68]; faster swimming sperm are more likely to reach and fertilize the egg. However, in many cases AI is performed using freeze-thawed samples. Cryopreservation of sperm has been shown to decrease sperm motility and increase DNA damage[69–71], decreasing the chance of successful fertilization. Previous studies have shown the use of red laser light to improve sperm swimming speed in vitro for a variety of animal species[33,43,59,63] and this method was shown to be safe in human sperm DNA[72]. However, lasers are costly and, depending on the spot size, may only be able to irradiate a small area at a time. A potential low-cost higher-throughput alternative to laser irradiation is light emitting diode (LED) irradiation.

The San Diego Zoo Institute for Conservation Research houses over 10000 samples of frozen animal cell cultures, sperm, eggs, and embryos in their "Frozen Zoo". The organization can benefit from novel, inexpensive, easy-to-use reproductive technologies to aid in conservation research. Many current assisted reproductive techniques are costly and require extensive training to perform. To combat this, a red light delivery device, referred to here as Sperm Motility Assisted Reproductive Technology (SMART), was designed to improve sperm motility to aid in the success of AI for endangered species. The design goals of the device include portability and cost-effectiveness to cover a wide range of applications beyond assisted reproduction.

3.2 Materials and Methods

3.2.1 LED array

An array of 36 635 nm little dot SMD LEDs (superbrightleds.com, St. Louis, MO) were arranged on a stripboard (Figure 3.1). The wires of the LEDs were soldered to a PCB and powered by a 12V power supply (Mean Well, Fremont, CA). LEDs were spaced 2 mm apart to cover an area of 58 mm x 58 mm. The maximum achievable power density above each LED was estimated using the inverse square law to yield the following equation

$$PD = \frac{P}{z^2} + n\left(\frac{P}{z^2 + r^2}\right) \tag{3.1}$$

where *PD* is the power density above the LED, *z* is its distance from the surface, *r* is the spacing between LEDs, *P* is the power output of one LED (estimated based on available product information), and *n* is the number of adjacent LEDs. Using this method, the maximum power density was calculated to be about 100 mW/cm^2, but it was assumed that much of the power would be lost to diffusion and scattering. It was assumed that LEDs

placed diagonally from an LED would have a negligible effect on the power density directly above it.

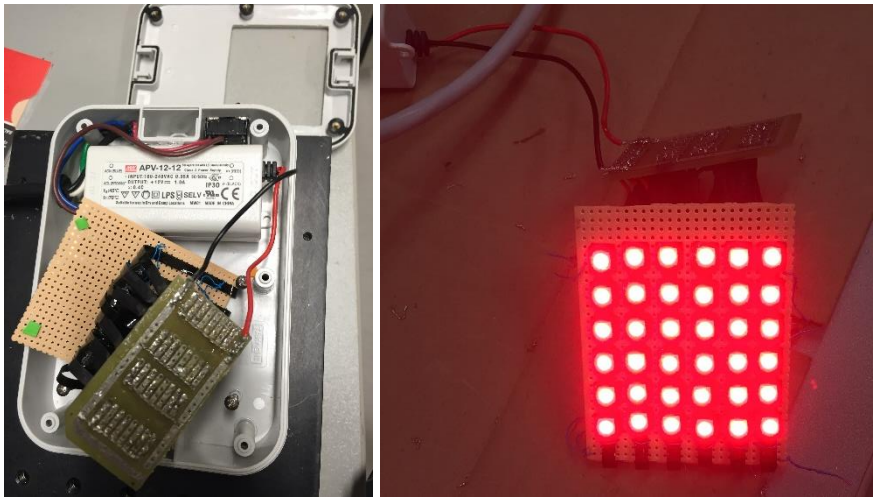

Figure 3.1. Circuitry and LED array used for red light device.

3.2.2 Enclosure

The LED array was encased in an ASA waterproof enclosure (Takachi, Chicago, IL). A waterproof enclosure was chosen to protect the electrical components from moisture, particularly for use in an incubator as the user may require that samples are irradiated at controlled temperatures. A 7.4 cm x 6.7 cm rectangle was cut out of the top of the encasing and a rectangle of ground glass (Edmund Optics, Barrington, NJ) of the same dimensions, 1.6 mm thick, was placed for diffuse light distribution to the sample. Clear silicone sealant was applied to the glass-plastic interface to maintain waterproofing. A schematic of the device is shown in Figure 3.2.

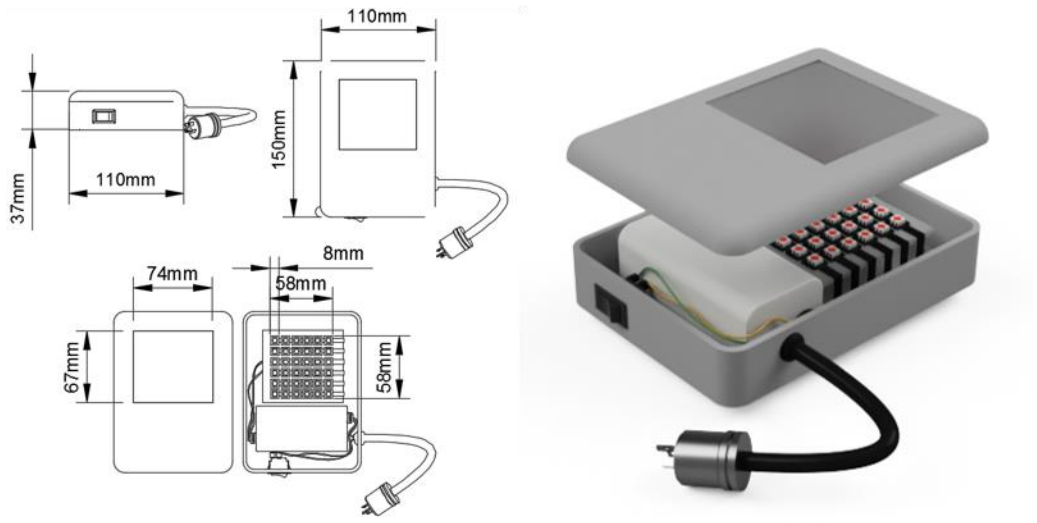

Figure 3.2. AutoDesk Fusion 360 models of the proposed red light device.

Figure 3.3. Fully assembled device.

3.2.3 Analysis of motility

Sperm VCL in response to irradiation from the device was assessed. Human sperm were prepared as described in Chapter 2. Two 6 µL aliquots were prepared in 20 µm 2-chamber slides (Leja, Netherlands). One aliquot was placed on the red light device while the other was kept in darkness. Due to the method of irradiation, sperm could not be imaged directly under red light illumination and tracked with the algorithm described in Chapter 2. Instead, VCL was measured using the IVOS CASA system (Hamilton Thorne, Beverly,

MA). The VCL of each aliquot was measured every 4 minutes, with a different aliquot measured every 2 minutes, for 50 minutes. Statistical significance was determined using a Student's t-test in R software (version 3.2.0).

3.2.4 Characterization of LED array

The power density of the emitted light as well as potential heat generation were evaluated. To determine the power density across the surface of the device, a power meter (Newport 918D-SL-OD3R, Irvine, CA) was used to take measurements at discrete xy-positions 1 mm above the surface. To determine whether heat was being generated by the power supply a thermistor was attached to the plastic surface of the device adjacent to the power supply. Temperature measurements were recorded every 15 seconds for 36 minutes. To determine whether heat was being generated by the LED array, a thermistor was attached to the glass surface of the device. Temperature measurements were recorded every 15 seconds for 45 minutes.

3.3 Results

3.3.1 Swim velocity following red light irradiation

The effect of 50 minutes of red LED irradiation on sperm VCL is shown in Figure 3.4. A significant increase in sperm VCL of about 15% was observed in the irradiated sample compared with the untreated sample after 20-40 minutes of irradiation, as measured with a Student's t-test ($p < 0.05$). Although the VCL of the irradiated sperm were also greater after 10-20 minutes and after 40 minutes, the difference in VCL was not statistically significant.

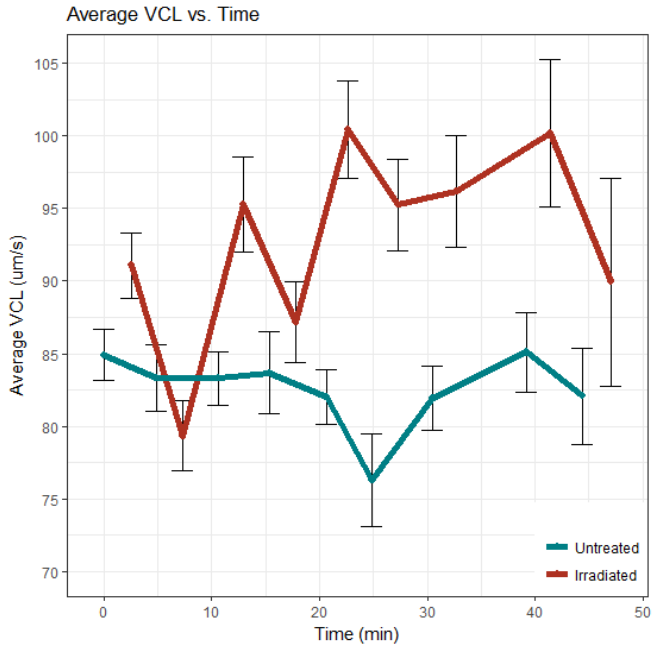

Figure 3.4. Comparison of sperm VCL during LED irradiation and without irradiation. Error bars indicate standard error.

3.3.2 Power density above LED array

The average power density across the array was determined to be 2.78 mW/cm^2 with a maximum of 3.49 mW/cm^2. The power density at each measured position is shown in Figure 3.5**.** Although the power density has small fluctuations at the center of the array, there is a sharp decline towards the edges of the LED array.

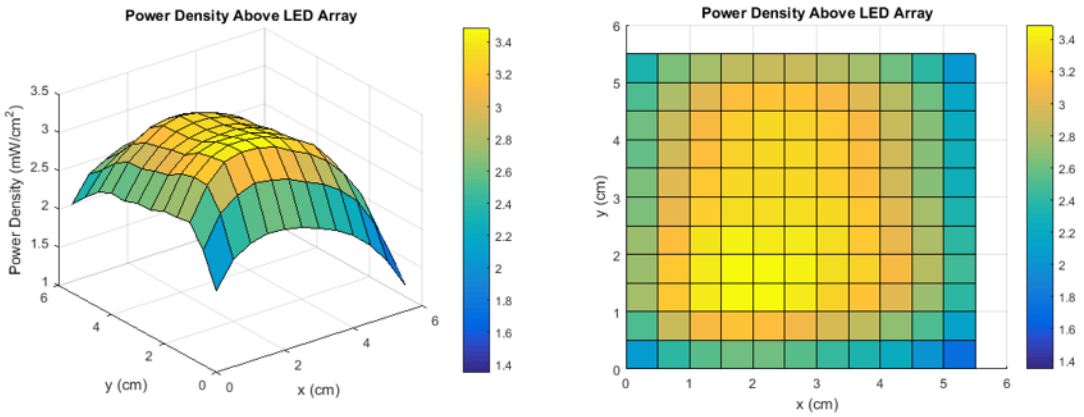

Figure 3.5. Power density above LED array measured at discrete positions above the array.

3.3.3 Temperature change over time

The temperatures at different locations of the device were measured over time. Plots of these measurements are shown in Figure 3.6. The glass surface exhibited temperatures exceeding physiological conditions after 18 minutes.

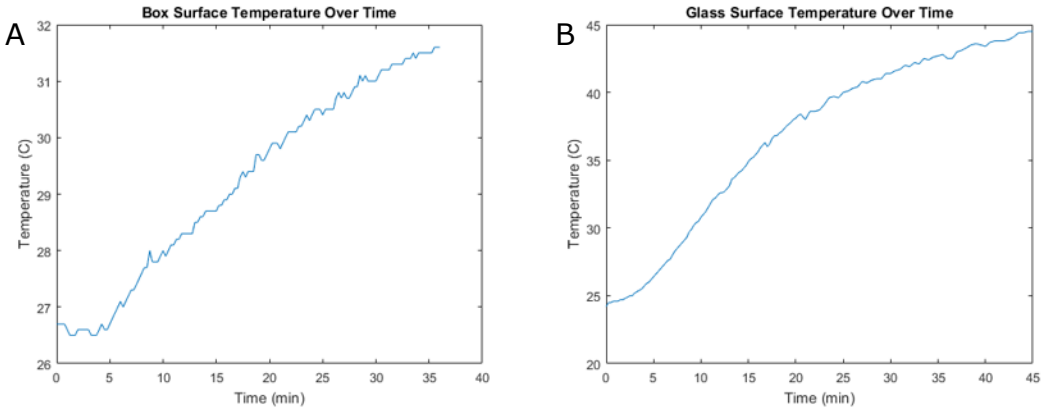

Figure 3.6. Temperature of (A) the plastic surface of the device and (B) the glass surface of the device over time.

3.4 Discussion

An inexpensive, easy-to-use device has been designed and tested to improve sperm swimming speed in vitro. Due to the wide window on the device, larger samples can be irradiated at a time, compared with the single-sample setup described in Chapter 2 (i.e. irradiation of 6-well dishes instead of irradiation of single dishes). The size of the LED array and corresponding window can be changed in future designs, if needed. The power density of the produced LED array was lower than the power density of the laser used in Chapter 2 but was shown to produce similar increases in swimming speed. Due to the decreased intensity of light, it may also be assumed that LED irradiation does not induce significant levels of oxidative DNA damage.

Future design goals include implementing a thermal management system as well as homogenizing the field of light produced by the LED array. From Figure 3.6, it appears

that there is heating from the LED array transmitted through the glass window that may be damaging to spermatozoa after long periods of time. Although motile spermatozoa were still observed during the duration of speed measurement, it is important that the heat be sequestered away from the sample while maintaining the delivery of photonic energy to the sample. This may be done by implementing a heat sink to conduct thermal energy away from the sample or adding cooling vents and a fan to circulate and remove warmer air. These were not implemented in this design due to unexpected space limitations and concerns with waterproofing. It is also possible that the increase in temperature contributed to the increase in swimming speed; design changes are being implemented to mitigate the effects of heating. For better homogenization of the power density above the LED array, resistors can be added to modulate the intensity of each LED. This will ensure even delivery of light to all spermatozoa in all irradiated samples. Another possibility is to add layers of diffusive material over the LED array. However, this may significantly scatter and decrease luminous flux on the sample. The device is currently being developed further to address these initial design issues.

Previous studies have analyzed the effect of red LED irradiation of fresh spermatozoa from humans[47,61] and boars[32] and noted improvements in VCL. It is important to note that in the present study, red LED irradiation was applied to frozen-thawed samples. In animal conservation applications, many samples are frozen-thawed to facilitate the spread of genetic diversity[65]. However, many assisted reproductive technologies in humans are conducted using fresh samples. Therefore, the described method should be applied to both fresh and frozen samples to ensure general effectiveness.

Future studies will include testing the device on various species of animal sperm. Because the device was originally designed for the San Diego Zoo Institute of Conservation Research, the main goal of this technology is to develop a fertility treatment that works on a wide variety of species to overcome the large diversity in animal reproductive biology. This technology also has implications beyond reproductive biology and can be used for other LLLT applications, such as wound healing, dermatology, and neurophysiology. Future iterations of the current device will be developed with these other applications in mind.

Acknowledgements

This material is based upon work supported by the Air Force Office of Scientific Research under award number FA9550-17-1-0193.

Chapter 4: The Effect of Red Light Irradiation on Optically Trapped Spermatozoa

4.1 Introduction

Although large numbers of thorough studies of spermatozoa quality and characteristics have been conducted, there is still much that is unknown about sperm motility. Conventionally, percentages of motile sperm, swimming speed, and sperm trajectories have been used as measures of sperm fitness. Sperm swimming force and tail beat frequency (TBF) are additional metrics for sperm quality, both of which are highly dependent on the energy dissipation of individual sperm. Increased sperm competition has been correlated with higher swimming force; it is implied that higher swimming force is indicative of increased ability to out-compete other sperm for successful fertilization[73]. TBF describes the frequency of tail movement for a single sperm. An increase in TBF was observed in response to incubation with pentoxyfilline[74], a phosphatase inhibitor that has been shown to increase sperm swimming speed and swimming force[75].

It has been suggested that sperm swimming force is instrumental in fertilization of the egg. Sperm must be able to penetrate both the cumulus oophorus, a layer of cells surrounding the oocyte, and the zona pellucida, where fertilization occurs. Although the sperm acrosome contains enzymes to help digest the cumulus oophorus, it has been shown that mammalian sperm are capable of penetrating the egg without them[76,77], indicating the importance of mechanical force. Additionally, it has been shown that surface receptors on the sperm interact with ligands on the zona[78]. In order to penetrate further into the egg, the sperm must be able to disrupt this ligand-receptor interaction[79]. Another study correlated the swimming force of epididymal sperm with fertilization[80] wherein it was shown that

sperm with lower swimming force produced fewer embryos, implying a positive correlation between swimming force and fertilization potential.

Studies have indicated a positive correlation between sperm swimming speed and swimming force[73,81]. Recently, it has been shown that red light irradiation of sperm can increase curvilinear velocity (VCL)[32,72]. One proposed mechanism for this increase is stimulation of cytochrome c oxidase (Cox), Complex IV of the electron transport chain. It has been shown to be a photoacceptor for red and near-IR light[51]. The absorption of these wavelengths is believed to cause an increase in ATP production, and thus an increase in VCL. It is therefore possible that an increase in VCL by 633 nm laser irradiation may also cause an increase in sperm swimming force, which may be of benefit to reproductive medicine particularly in increasing fertilization potential.

In the current work, the effect of red light illumination on optically trapped spermatozoa is described. The average force exerted by the sperm and tail beat frequency were determined in the optical trap by observing the time dependent position of the sperm head in the optical trap under red light.

4.1.1 Measuring sperm tail beat frequency

The widely used CASA system does not measure individual sperm tail frequencies, but instead measures cross-beat frequency. This is a measure of the aggregate vibrational frequency of all of the sperm in the field of view. The image acquisition rate may also have an effect on the measured frequencies. Especially for fast sperm with nonlinear trajectories, high frequency data acquisition is necessary for accurate measurements[82]. However, CASA systems typically operate at a maximum of 30-60 frames per second, which may be

insufficient to capture fine movements such as TBF. Therefore, different methods should be employed for accurate TBF measurement.

Another more direct method of measuring TBF was proposed by Chen et al. Sperm heads were stuck to glass slides with their tails free. A flash lamp was designed for use with a light microscope to flash at the same frequency as tail movement based on measurable vibrational sperm movement[74]. The measured frequency was verified based on timestamped images acquired as the lamp flashed. Although this methodology eliminates the need for complicated calculations and consideration of external sources of vibrational movement, it is possible that the bright flash lamp may affect sperm motility. Therefore, it is desirable to measure tail beat frequency using methods that do not bias measurements. One solution is to determine frequencies based on position data and generating the power spectral density (PSD) from the acquired signal. Because the majority of sperm movement comes from tail movement, the peak in the power spectrum corresponds with the tail beat frequency.

4.1.2 Measuring forces generated by sperm cells

The forces exerted by individual sperm are difficult to measure due to their small size and inherent motility. Baltz et al. used the forces generated by a suction micropipette to measure sperm escape force[79]. The suction force was lowered by decreasing the pressure within the pipette until the sperm was able to escape. The sperm swimming force was then calculated from the escape pressure and the area of the pipette opening. However, this method requires that only the sperm head is captured laterally on the pipette during force measurement, causing only about 20 in 10000 sperm to be measured.

Sperm swimming forces can also be measured by optically trapping sperm. One method to determine the force exerted by the sperm is to lower the trap power until the sperm is able to escape[73,81]. The force can then be calculated from the escape power by the following relationship

$$F_{esc} = Q\frac{n\,P_{esc}}{c} \tag{4.1}$$

where P_{esc} is the trap power at which the sperm escapes the trap, c is the speed of light, n is the refractive index of the medium, and Q is the geometrically determined trapping efficiency parameter, determined to be 0.12 for ellipsoid human sperm oriented longitudinally[27]. Although this method is a simple, mathematically inexpensive method of determining swimming force, it has some drawbacks. For example, it does not account for directionality of force. It also relies on a single measurement obtained per sperm at a single instance in time without being able to take into account direction, position, or amount of sperm movement prior to escape. Confined sperm are not necessarily exerting the same amount of force at any given time. However, this method does preserve the integrity of the sperm cells by only exposing them to radiation for a small amount of time, thus reducing the possibility of "opticution" and allowing for high throughput measurements.

Another way of determining force is by its relation with the optical trap stiffness. Because optical traps can be approximated as a parabolic potential well, the trapping force can be calculated from Hooke's law

$$F = \kappa x \tag{4.2}$$

with trap stiffness, κ, as the proportionality constant, defined for a trapped particle under Brownian motion via equipartition theory as[28]

$$\kappa = \frac{k_b T}{< x^2 >} \tag{4.3}$$

In the current chapter, sperm dynamics in the optical trap are used to generate a force metric which can serve as a measure of the overall forces present in differing populations of sperm.

4.2 Materials and Methods

4.2.1 Sample preparation

Cryogenically frozen human sperm samples obtained from Infertility, Gynecology, and Obstetrics Medical Group (San Diego, CA) were collected from healthy men and frozen according to standard freezing protocol[49,50]. Samples were thawed in a water bath at 37°C before centrifugation at 208g for 10 minutes. The pellet was then resuspended in 1 mL modified human tubal fluid (HTF) (Irvine Scientific, Irvine, CA) with 5% serum substitute supplement (SSS) (Irvine Scientific) and centrifuged again. This wash technique was performed twice for every sample used for a final concentration of about 30000 sperm/mL. 10 μL of the suspension was plated in a 35 mm glass bottom dish with 2mL of modified HTF. To minimize the effect of diminishing motility over time, samples were discarded within 3 hours of preparation.

4.2.2 Optical setup

Motile spermatozoa were optically trapped in a single beam gradient trap before and after red light irradiation. An Nd:YVO_4 continuous wave 1064 nm wavelength laser (Spectra Physics, BL-106C, Mountain View, CA) was used as the trapping beam. After power attenuation, the beam was directed through a 4f imaging system and into an Axiovert S100 2TV microscope (Zeiss, Thornwood, NY) and a 63x NA 1.4 phase III oil immersion

objective (Zeiss) (transmission ≈25% at 1064 nm). Samples were trapped at a power of 150 mW, at the focal spot. For red light irradiation, samples were irradiated from above using a 633 nm He-Ne laser light source (Intense 7404, North Brunswick, NJ) coupled to a multimode, homogenizing fiber (Medlight FD, Switzerland) at a power density of 31 mW/cm^2 for 30 minutes. Experiments were conducted in the absence of excess lighting to prevent the effect of other wavelengths of light. Images were taken using a CMOS camera (Allied Vision, Mako G-030, Germany) at approximately 500 frames per second. A diagram of the optical setup can be seen in Figure 4.1.

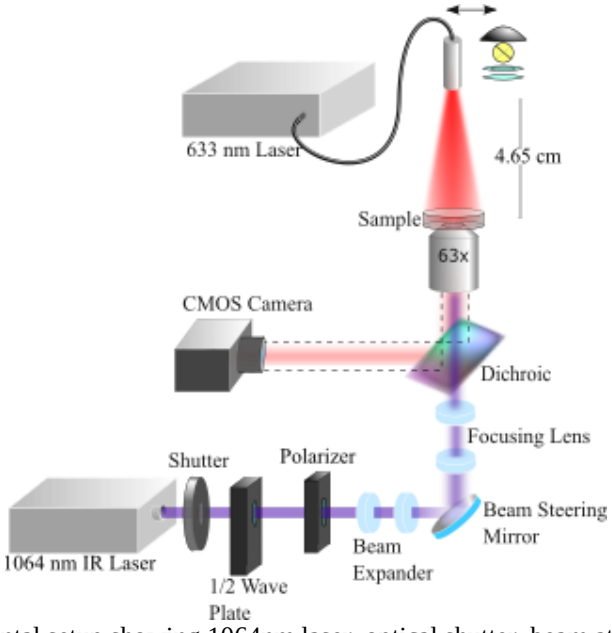

Figure 4.1. The experimental setup showing 1064nm laser, optical shutter, beam attenuation and 4f imaging system for optical tweezers and dichroic mirror, and camera for high speed imaging of sperm position.

4.2.2 Sperm position analysis

Sperm within the optical trap were tracked over a maximum duration of 20 seconds to avoid photo damage using center of mass (COM) tracking implemented in LabVIEW. The image is thresholded to eliminate background pixels and COM is computed via the formula:

$$x_{center} = \frac{\sum xPix}{\sum Pix} \tag{4.4}$$

$$y_{center} = \frac{\sum yPix}{\sum Pix} \tag{4.5}$$

where *Pix* is the pixel value in the image and *x* and *y* are coordinates in the image plane. Though it is possible to use this algorithm to track in three dimensions, only the x and y dimensions are tracked here to reduce complexity[83].

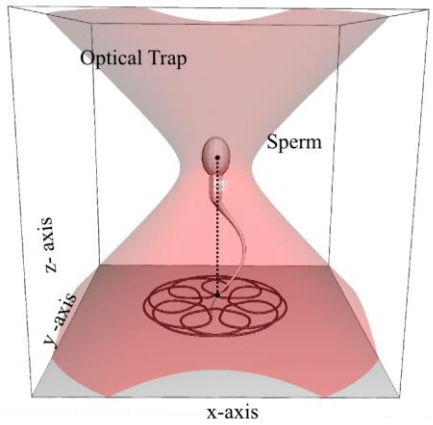

Figure 4.2. Representation of sperm in the optical trap. Over short time scales the sperm traces out a "rose curve" like trajectory in the xy-plane.

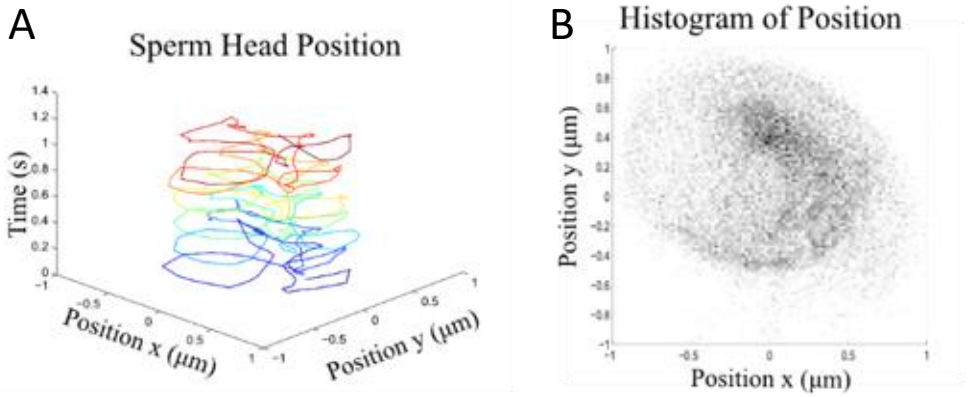

Figure 4.3. Histogram of sperm movement. (A) Trajectory of the sperm head in the xy-plane over a 1 second interval. (B) 2D histogram of sperm head position. Dark areas represent a greater number of counts in that location.

Empirically, it was found that the trapped sperm traces a "rose curve" like trajectory in the xy-plane i.e. one which resembles a sine wave in polar coordinates, shown in Figure

4.2. This is due to the elliptical motion of the sperm head caused by flagellar motion as the sperm tries to escape the optical potential. Brownian noise and stochastic reorientations serve to perturb this behavior causing the ensemble position data to be largely Gaussian in distribution despite the periodic oscillations of the sperm head. Figure 4.3 illustrates this by showing a time sequence of sperm motion in the xy-plane and the position histogram of the sperm head taken over 10 seconds. Without a rigorous mathematical model of this behavior it is difficult to predict the dynamics of the sperm head in the optical trap nor is it within the scope of the current study. Instead the notion of an optical pseudo-potential is adopted[84]. Because the trap stiffness is a property of the geometry of the optical trap and of the trapped particle, there may be variation in trap stiffness due to particle orientation. This can be accounted for by measuring the trap stiffness for immotile sperm over a range of orientations and averaging over the occupation probability of each orientation state. The extra energy imparted into the system by the motion of the flagella can therefore be quantified by observation of the variations of the mean squared displacement (MSD) between different sperm.

The relative force imparted by the optical trap can be estimated using Eqn. (4.2) and Eqn. (4.3). The trapping force is then approximately proportional to the square root of MSD, which represents an average net displacement over the duration of measurement. Since the instantaneous velocity of the sperm is found empirically to average to zero at all points in the xy-plane, the MSD due to the motion of the sperm cell can be approximated as proportional to the force exerted by the sperm.

4.3 Results

4.3.1 The effect of red light on TBF and PSD

The power spectral densities for 31 non-irradiated and 43 irradiated sperm were plotted and the peak frequencies determined from the xy-position data. The frequencies that occur at the highest power (indicated as the x-coordinate of the black squares in Figure 4.4) correspond to the frequency of sperm tail beat. High-frequency, low power information represents Brownian noise. From these plots, there is small variation in both frequency and power at that frequency. However, it was determined that these differences were not statistically significant ($p > 0.05$) (Figure 4.5).

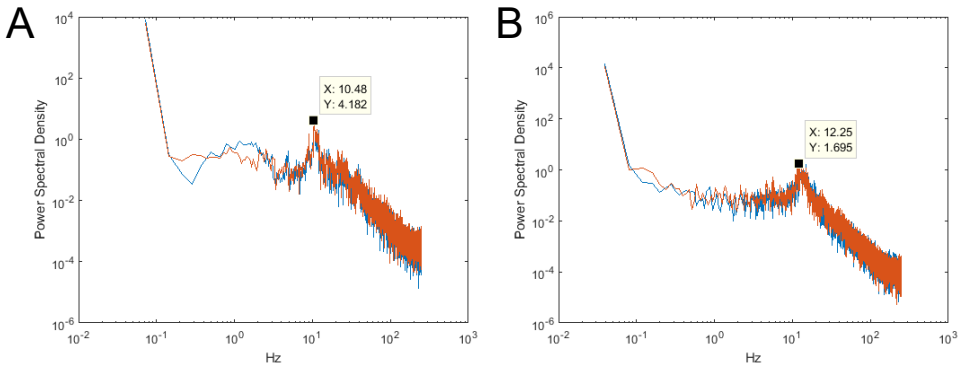

Figure 4.4. Power spectra of trapped spermatozoa (A) before irradiation and (B) after irradiation. Peak frequencies (black square) indicate approximate tail beat frequencies. Blue lines indicate x-coordinate data and orange lines indicate y-coordinate data.

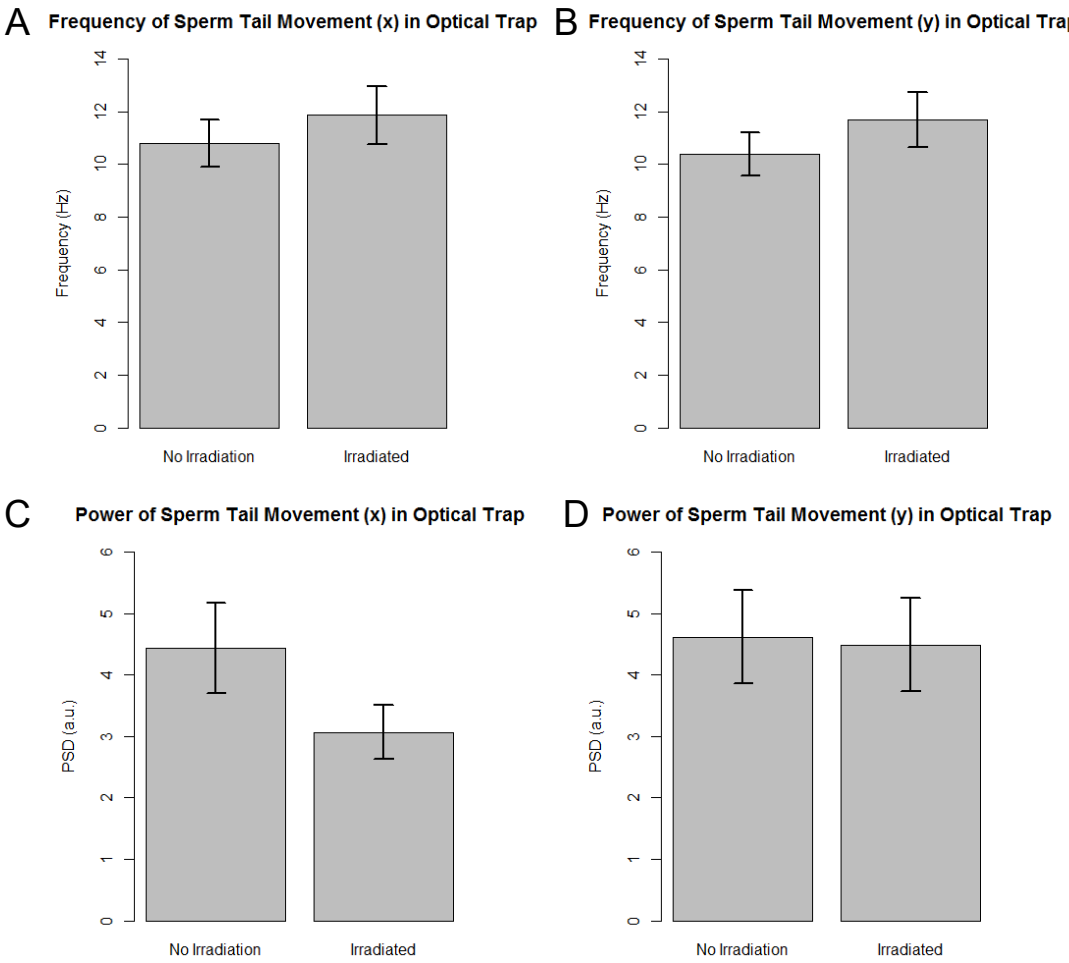

Figure 4.5. Analysis of power spectra for non-irradiated and irradiated spermatozoa. (A-B) Peak frequencies for x and y-coordinate information. (C-D) Power at peak frequencies for x and y-coordinate information. Error bars indicate standard error. The differences shown were not found to be statistically significant ($p > 0.05$).

4.3.2 Trap stiffness

Assuming a symmetric ellipsoid distribution, the trap stiffness for different rotational orientations of trapped sperm can be determined. Rotational orientations were determined by mapping the length of an imaged sperm to an orientation based on measured lengths in axially and laterally oriented sperm. A schematic of this process is shown in Figure 4.6. Approximately 2000 images of a single trapped sperm were analyzed and a Gaussian fit was applied to the histogram of orientations to produce a probability density

function representative of the occupation probability of each orientation (Figure 4.7). Trap stiffness was determined from the MSDs of 5 immotile sperm trapped axially and 2 trapped at about 65° determined using the method described above. The trap stiffness when sperm were in the axial position was estimated to be 10.32 ± 4.04 pN/μm and 10.83 ± 5.57 pN/μm at 65°. Extrapolating these estimated values to an ellipsoid distribution yielded the values shown in Figure 4.8. Weighted averaging yielded a trap stiffness of 10.68 pN/μm.

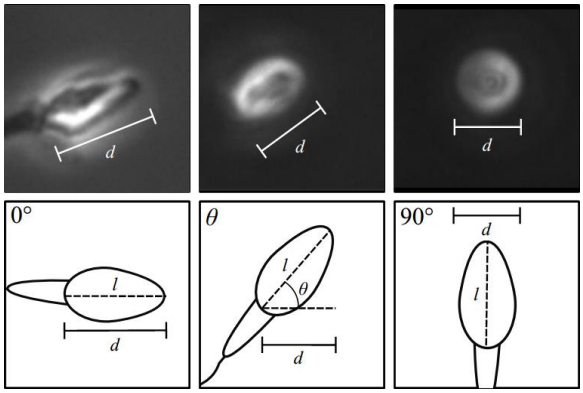

Figure 4.6. Determination of rotational orientation of optically trapped spermatozoa. The length of the sperm head (*l*) was measured for sperm stuck to a cover slip. The major axis of the trapped sperm head (*d*) was measured using LabVIEW. The orientation angle was then determined based on trigonometry. For laterally oriented sperm heads (0°), *d* = *l*. For axially oriented sperm heads (90°), *d* is equal to the width of the sperm head.

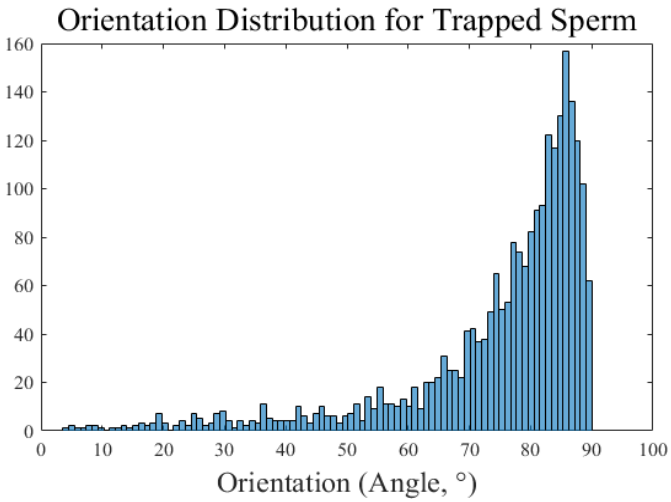

Figure 4.7. Occupation probabilities of each rotational orientation of trapped sperm heads. This histogram was generated based on orientations measured using the method described above for a motile trapped sperm over about 2000 frames.

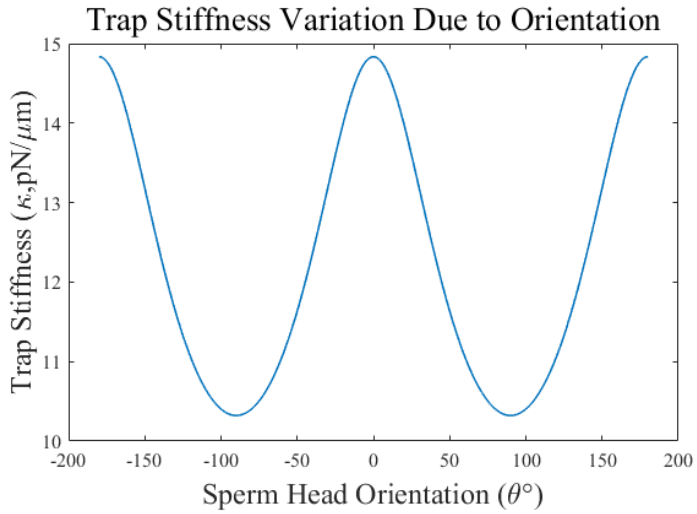

Figure 4.8. Estimated trap stiffness for different rotational orientations of sperm heads.

4.3.3 The effect of red light on MSD

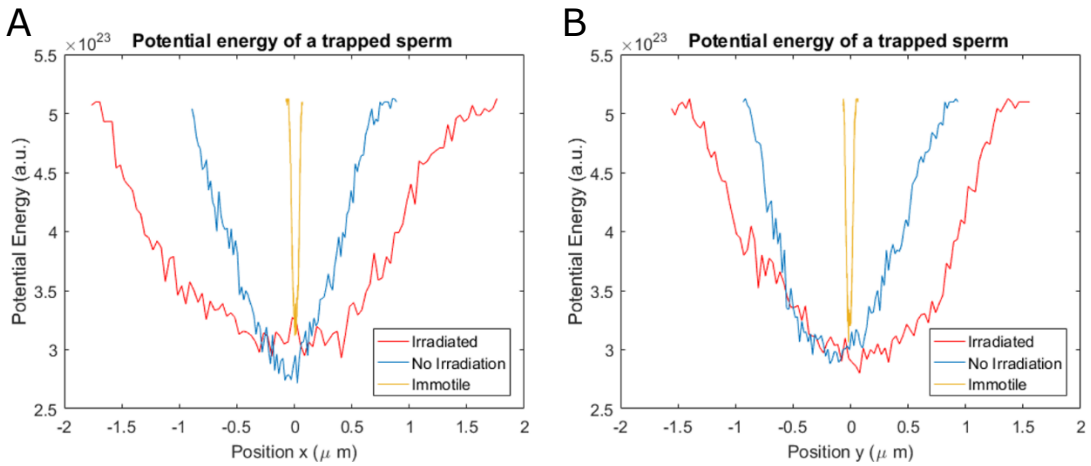

Figure 4.9. Comparison of potential energy for irradiated, non-irradiated and immotile sperm calculated via optical potential analysis (A) in the x-direction and (B) in the y-direction.

From the position data, the relative potential energies of sperm with and without irradiation were calculated using Boltzmann statistics. Figure 4.9 compares the distributions of potential energy over position for irradiated, non-irradiated, and immotile sperm. The potentials for the trapped sperm appear parabolic with or without red light irradiation with low potential energy in the middle of the potential well and high potential

energy at the edges. The potential distribution shows how confined the sperm head is to the center of the trap. The less the sperm is able to move, the narrower the parabola.

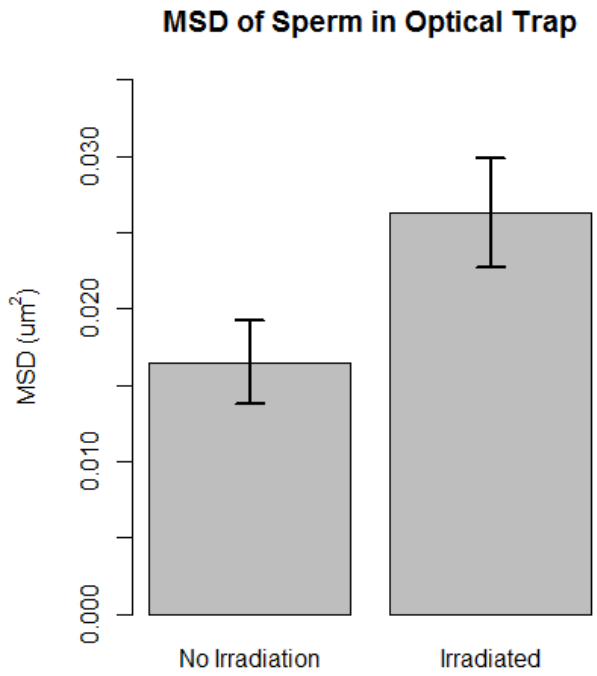

Figure 4.10. MSD of trapped spermatozoa with and without red light irradiation. Error bars represent standard error. The data were found to be statistically significant ($p = 0.01269$).

The MSDs for 31 motile sperm before red light irradiation and 43 motile sperm after red light irradiation were measured. Although more sperm were trapped, data were excluded if (a) a second sperm entered the trap, (b) the sperm swam out of the trap before position data was attained, or (c) a histogram of the sperm position indicated tracking errors. Sperm had an average MSD of 0.026 μm^2 and 0.016 μm^2 with and without red light irradiation, respectively (Figure 4.10). From the estimated average trap stiffness, this produces trapping forces of 1.76 pN and 1.38 pN with and without red light irradiation, respectively. A Shapiro-Wilk test indicated that the distributions of MSD data were non-normal. Thus, a Kruskal-Wallis test was used to compare the two groups. The increased MSD in the irradiated group was found to be statistically significant ($p < 0.05$).

4.4 Discussion

MSD is a measure of the average squared distance a particle undergoing random motion has traveled. As such, MSD is representative of aggregate displacement over time and is highly correlated with optical trapping force. Thus, a larger MSD is indicative of a higher trapping force necessary to hold a particle in place. The irradiated sperm in this study had a larger MSD than the untreated sperm, implying greater relative swimming force in the irradiated sperm. It should be noted that the equipartition theory holds for systems in equilibrium, which motile sperm are not. Therefore, the force measurements presented here are qualitative values intended for the comparison of spermatozoa in different states. More robust numerical analysis and modeling is required for an accurate quantitative measure of swimming force.

Due to their nonuniform shape, sperm head position data may be prone to error through COM tracking, as it relies on the pixel intensities within an image. In order to track positions of particles, images must be thresholded to produce a binary image wherein the tracked object is completely distinct from the background. Although computationally inexpensive, this method is unable to take into account the effects of asymmetrical objects rotating within optical traps. Other tracking techniques such as cross-correlation based algorithms may provide a more accurate measure of cell position[85]. However, because they require more computational time, this method was not utilized in the current work. The study outlined here relies on large data sets, limited by camera frame rate and image processing time. The current methodology was necessitated by the relatively short time window over which useful statistical data could be gathered.

Although a slight increase in tail beat frequency was observed in response to red light irradiation, this increase was not statistically significant. It was initially hypothesized that an increase in sperm swimming speed would produce a similar increase in tail beat frequency, as sperm movement is controlled by the flagellum. It is likely that the method of position-tracking of the sperm head and analyzing the power spectrum does not produce an accurate enough measure of tail beat frequency, since it is an indirect measurement. In some cases, multiple peaks in the power spectrum were observed, possibly due to contributions from other frequencies that were not accounted for. It is possible that the method described by Chen et al.[74] could be implemented without the use of a flash lamp (at the expense of image acquisition) for a more direct measure of tail movement. Another alternative is to correlate tail beat frequency with rotational frequency, rather than translational motion. Trapped spermatozoa tend to orient axially where translational motion is restricted, but rotational motion is not. Subramani et al. saw a positive correlation between rotational speed and sperm swimming speed in trapped sperm[86]. However, for more accurate measures of tail beat frequency, future experiments should focus on more direct measurements of tail motion.

It is possible that the 20 second trap duration could have adversely affected sperm motility. With a 1064 nm beam, significant decreases in VCL were observed after 45 seconds at 1 W for fresh human sperm (mean VCL ≈ 1-60 μm/s)[87] and after 15 seconds at 420 mW for fresh dog sperm (mean VCL ≈ 102 μm/s)[88]. It is possible that the observed decreases are velocity or species dependent. Further experiments should be conducted to verify whether frozen-thawed human sperm experience a decrease in VCL at the power

and duration used in this study. Nevertheless, optical trapping is a promising method of further sperm characterization.

Acknowledgments

Thank you to The San Diego Zoo Institute for Conservation Research, The Institute for Engineering in Medicine at UC San Diego, The Beckman Laser Institute at UC Irvine, and Dr. Veronica Gomez-Godinez. This material is based upon work supported by the Air Force Office of Scientific Research under award number FA9550-17-1-0193. Portions of this work were presented at the OSA Biophotonics Congress in 2017 (paper OtTu2E.3).

Chapter 4, in part, is a reprint of the material published as it appears in "Effect of red light on optically trapped spermatozoa" by K.W. Chow, D. Preece, M.W. Berns. *Biomed. Opt. Express* **8,** 4200-4205 (2017). The thesis author was the first author of this material.

Chapter 5: Conclusions

In this thesis, the efficacy of 633 nm red laser light at a power density of 31 mW/cm^2 in improving spermatozoa quality, as measured in terms of increase in curvilinear velocity (VCL) and swimming force as well as preservation of DNA integrity were demonstrated. An increase in VCL of 17-47% was observed after 35 minutes of laser irradiation at a power density of 5.66 mW/cm^2, measured using a novel wavelet-based tracking algorithm. Swimming force was estimated using mean squared displacement (MSD) of optically trapped sperm following 30 minutes of red light irradiation. MSD was observed to increase from 0.016 μm^2 to 0.026 μm^2 following irradiation. This correlates with an approximate increase in swimming force from 1.38 pN to 1.76 pN. DNA integrity following irradiation was characterized by measuring γH2AX and 8-oxo-G formation, both of which have been shown to be indicators of oxidative stress. It was determined that there were no significant increases in either DNA damage marker when compared with an untreated control. Based on these findings, a device for the in vitro LED irradiation of spermatozoa was designed and constructed and showed increases in VCL similar to those seen following laser irradiation after 20-40 minutes. This device is being further developed to be used in animal conservation research at the San Diego Zoo.

Low-level laser therapy has potential applications in assisted reproductive technologies in addition to the more established applications in dermatology, wound healing, and dentistry. However, a clear mechanism for the therapeutic effects of red light has yet to be elucidated. The mechanisms that have been proposed for wound healing, angiogenesis, and inflammation involve the stimulation of surrounding immune cells and

increased gene transcription. Because spermatozoa do not produce proteins and are treated in vitro, the same mechanisms may not be applicable in sperm. A number of studies have been conducted to trace Ca^{2+} uptake and mitochondrial membrane potential in sperm. Additional studies may benefit from the extraction of mitochondria from irradiated and non-irradiated sperm to compare ATP content. However, because sperm mitochondria are coupled to one another, they are difficult to isolate from the midpiece[21,89]. Alternatively, ATP can be extracted and quantified directly[90]. Such studies may further validate the application of LLLT for fertility treatments.

It was observed that red light irradiation increases sperm motility parameters such as curvilinear velocity and swimming force. These qualities have been associated with increased reproductive success. Further studies should be conducted to confirm whether the improvements resulting from red light irradiation also correlate positively with fertilization rates. Since sperm morphology and energetics are significantly different between species, the effect of photo-stimulation could also vary significantly for different species. This methodology should be applied to a wider variety of species to confirm the scope of its utility. Nevertheless, the potential of red light irradiation in fertilization is demonstrated.

References

1. Cummins, J. M. and Woodall, P. F. On mammalian sperm dimensions. *J. Reprod. Fertil.* **75,** 153–175 (1985).

2. Wassarman, P. M. Zona pellucida glycoproteins. *J. Biol. Chem.* **283,** 24285–24289 (2008).

3. Van Soom, A., Tanghe, S., De Pauw, I., Maes, D., and De Kruif, A. Function of the cumulus oophorus before and during mammalian fertilization. *Reprod. Domest. Anim.* **37,** 144–151 (2002).

4. de Lamirande, E. and O'Flaherty, C. Sperm activation: Role of reactive oxygen species and kinases. *Biochim. Biophys. Acta - Proteins Proteomics* **1784,** 106–115 (2008).

5. Salman Yazdi, R., Bakhshi, S., Jannat Alipoor, F., Akhoond, M. R., Borhani, S., Farrahi, F., Lotfi Panah, M., and Sadighi Gilani, M. A. Effect of 830-nm diode laser irradiation on human sperm motility. *Lasers Med. Sci.* **29,** 97–104 (2014).

6. Qi, H., Moran, M. M., Navarro, B., Chong, J. A., Krapivinsky, G., Krapivinsky, L., Kirichok, Y., Ramsey, I. S., Quill, T. A., and Clapham, D. E. All four CatSper ion channel proteins are required for male fertility and sperm cell hyperactivated motility. *Proc. Natl. Acad. Sci.* **104,** 1219–1223 (2007).

7. Farivar, S., Malekshahabi, T., and Shiari, R. Biological effects of low level laser therapy. *J. lasers Med. Sci.* **5,** 58–62 (2014).

8. Saltmarche, A. E. and Saltmarche, A. E. Low level laser therapy for healing acute and chronic wounds – the extendicare experience. *Int. Wound J.* **5,** 351–360 (2008).

9. Park, I.-S., Chung, P.-S., and Ahn, J. C. Enhancement of Ischemic Wound Healing by Spheroid Grafting of Human Adipose-Derived Stem Cells Treated with Low-Level Light Irradiation. *PLoS One* **10,** e0122776 (2015).

10. AlGhamdi, K. M., Kumar, A., and Moussa, N. a. Low-level laser therapy: A useful technique for enhancing the proliferation of various cultured cells. *Lasers Med. Sci.* **27,** 237–249 (2012).

11. Mester, A. Laser biostimulation. *Photomed. Laser Surg.* **31,** 237–239 (2013).

12. Spitler, R. and Berns, M. W. Comparison of laser and diode sources for acceleration of in vitro wound healing by low-level light therapy. *J. Biomed. Opt.* **19,** 38001 (2014).

13. Karu, T. I. and Kolyakov, S. F. Exact action spectra for cellular responses relevant to phototherapy. *Photomed. Laser Surg.* **23,** 355–361 (2005).

14. Passarella, S., Casamassima, E., Molinari, S., Pastore, D., Quagliariello, E., Catalano, I. M., and Cingolani, A. Increase of proton electrochemical potential and ATP synthesis in rat liver mitochondria irradiated in vitro by helium-neon laser. *FEBS Lett.* **175,** 95–99 (1984).

15. Wong-Riley, M. T., Bai, X., Buchmann, E., and Whelan, H. T. Light-emitting diode treatment reverses the effect of TTX on cytochrome oxidase in neurons. *Neuroreport* **12,** 3033–3037 (2001).

16. Pastore, D., Greco, M., and Passarella, S. Specific helium-neon laser sensitivity of the purified cytochrome c oxidase. *Int. J. Radiat. Biol.* **76,** 863–870 (2000).

17. Huang, Y.-Y., Nagata, K., Tedford, C. E., McCarthy, T., and Hamblin, M. R. Low-level laser therapy (LLLT) reduces oxidative stress in primary cortical neurons in vitro. *J. Biophotonics* **838,** n/a-n/a (2012).

18. Kingsley, J. D., Demchak, T., and Mathis, R. Low-level laser therapy as a treatment for chronic pain. *Front. Physiol.* **5,** (2014).

19. Ball, K. A., Castello, P. R., and Poyton, R. O. Low intensity light stimulates nitrite-dependent nitric oxide synthesis but not oxygen consumption by cytochrome c oxidase: Implications for phototherapy. *J. Photochem. Photobiol. B Biol.* **102,** 182–191 (2011).

20. Lubart, R., Friedmann, H., Cohen, N., and Breitbart, H. Effect of HeNe laser on calcium signals in sperm cells. in *EUROPTO Conference on Effects of Low-Power Light on Biological Systems* **3569,** 45–49 (1998).

21. Breitbart, H., Levinshal, T., Cohen, N., Friedmann, H., and Lubart, R. Changes in calcium transport in mammalian sperm mitochondria and plasma membrane irradiated at 633 nm (HeNe laser). *J. Photochem. Photobiol. B Biol.* **34,** 117–121 (1996).

22. Koppers, A. J., De Iuliis, G. N., Finnie, J. M., McLaughlin, E. a, and Aitken, R. J. Significance of mitochondrial reactive oxygen species in the generation of oxidative stress in spermatozoa. *J. Clin. Endocrinol. Metab.* **93,** 3199–3207 (2008).

23. Ashkin, A., Dziedzic, J. M., Bjorkholm, J. E., and Chu, S. Observation of a Single-Beam Gradient Force Optical Trap for Dielectric Particles. *Opt. Lett.* **11,** 288–290 (1986).

24. Neuman, K. C. and Block, S. M. Optical Trapping. *Rev. Sci.* **75,** 2787–2809 (2004).

25. Crocker, J. C. and Grier, D. G. Methods of Digital Video Microscopy for Colloidal Studies. *J. Colloid Interface Sci.* **179,** 298–310 (1996).

26. Liang, H., Wright, W. H., Cheng, S., He, W., and Berns, M. W. Micromanipulation of chromosomes in PTK2 cells using laser microsurgery (optical scalpel) in combination with laser-induced optical force (optical tweezers). *Experimental cell research* **204,** 110–120 (1993).

27. König, K., Svaasand, L., Liu, Y., Sonek, G., Patrizio, P., Tadir, Y., Berns, M. W., and Tromberg, B. J. Determination of motility forces of human spermatozoa using an 800 nm optical trap. *Cell. Mol. Biol. (Noisy-le-grand).* **42,** 501–509 (1996).

28. Gibson, G. M., Leach, J., Keen, S., Wright, A. J., and Padgett, M. J. Measuring the accuracy of particle position and force in optical tweezers using high-speed video microscopy. *Opt. Express* **16,** 14561–14570 (2008).

29. Amann, R. P. and Waberski, D. Computer-assisted sperm analysis (CASA): Capabilities and potential developments. *Theriogenology* **81,** 5–17 (2014).

30. Karu, T. I. Lasers in Infertility Treatment: Irradiation of Oocytes and Spermatozoa. *Photomed. Laser Surg.* **30,** 239–241 (2012).

31. Firestone, R. S., Esfandiari, N., Moskovtsev, S. I., Burstein, E., Videna, G. T., Librach, C., Bentov, Y., and Casper, R. F. The Effects of Low-Level Laser Light Exposure on Sperm Motion Characteristics and DNA Damage. *J. Androl.* **33,** 469–473 (2012).

32. Yeste, M., Codony, F., Estrada, E., Lleonart, M., Balasch, S., Peña, A., Bonet, S., and Rodríguez-Gil, J. E. Specific LED-based red light photo-stimulation procedures improve overall sperm function and reproductive performance of boar ejaculates. *Sci. Rep.* **6,** 22569 (2016).

33. Cohen, N., Lubart, R., Rubinstein, S., and Breitbart, H. Light irradiation of mouse spermatozoa: stimulation of in vitro fertilization and calcium signals. *Photochem. Photobiol.* **68,** 407–413 (1998).

34. Shahar, S., Wiser, A., Ickowicz, D., Lubart, R., Shulman, A., and Breitbart, H. Light-mediated activation reveals a key role for protein kinase A and sarcoma protein kinase in the development of sperm hyper-activated motility. *Hum. Reprod.* **26,** 2274–2282 (2011).

35. Chohan, K. R., Griffin, J. T., and Carrell, D. T. Evaluation of chromatin integrity in human sperm using acridine orange staining with different fixatives and after cryopreservation. *Andrologia* **36,** 321–326 (2004).

36. Aitken, R. J. and De Iuliis, G. N. Origins and consequences of DNA damage in male germ cells. *Reprod. Biomed. Online* **14,** 727–733 (2007).

37. Li, Z., Yang, J., and Huang, H. Oxidative stress induces H2AX phosphorylation in human spermatozoa. *FEBS Lett.* **580,** 6161–6168 (2006).

38. Mah, L.-J., El-Osta, a, and Karagiannis, T. C. gammaH2AX: a sensitive molecular marker of DNA damage and repair. *Leuk. Off. J. Leuk. Soc. Am. Leuk. Res. Fund, U.K* **24,** 679–686 (2010).

39. Rogakou, E. P., Pilch, D. R., Orr, A. H., Ivanova, V. S., and Bonner, W. M. DNA double-stranded breaks induce histone H2AX phosphorylation on serine 139. *J. Biol. Chem.* **273,** 5858–5868 (1998).

40. Wright, C., Milne, S., and Leeson, H. Sperm DNA damage caused by oxidative stress: Modifiable clinical, lifestyle and nutritional factors in male infertility. *Reprod. Biomed. Online* **28,** 684–703 (2014).

41. Ocaña-Quero, J. M., Gomez-Villamandos, R., Moreno-Millan, M., and Santisteban-Valenzuela, J. M. Biological effects of helium-neon (He-Ne) laser irradiation on acrosome reaction in bull sperm cells. *J. Photochem. Photobiol. B Biol.* **40,** 294–298 (1997).

42. Dreyer, T. R., Siqueira, a. F. P., Magrini, T. D., Fiorito, P. a., Assumpção, M. E. O. a., Nichi, M., Martinho, H. S., and Milazzotto, M. P. Biochemical and topological analysis of bovine sperm cells induced by low power laser irradiation. *Med. Laser Appl. Laser-Tissue Interact. V* **8092,** 80920V--80920V--7 (2011).

43. Iaffaldano, N., Paventi, G., Pizzuto, R., Passarella, S., Cerolini, S., Zaniboni, L., Marzoni, M., Castillo, A., and Rosato, M. P. The post-thaw irradiation of avian spermatozoa with He-Ne laser differently affects chicken, pheasant and turkey sperm quality. *Anim. Reprod. Sci.* **142,** 168–172 (2013).

44. Nicolae, D., Stela, Z., Hortanse, A. A., Irina, T., Iaffaldano, N., Paventi, G., and Dragomir, C. Study on the effects of exposure to different doses of energy generated by a He-Ne laser on the quality of frozen-thawed semen of ram. *Rom. Biotechnol. Lett.* **20,** 10381–10387 (2015).

45. Iaffaldano, N., Rosato, M. P., Paventi, G., Pizzuto, R., Gambacorta, M., Manchisi, A., and Passarella, S. The irradiation of rabbit sperm cells with He-Ne laser prevents their in vitro liquid storage dependent damage. *Anim. Reprod. Sci.* **119,** 123–129 (2010).

46. Fernandes, G. H. C., De Tarso Camillo De Carvalho, P., Serra, A. J., Crespilho, A. M., Schatzman Peron, J. P., Rossato, C., Leal-Junior, E. C. P., and Albertini, R. The effect of low-level laser irradiation on sperm motility, and integrity of the plasma membrane and acrosome in cryopreserved bovine sperm. *PLoS One* **10,** 1–11 (2015).

47. Salama, N. and El-Sawy, M. Light-emitting diode exposure enhances sperm motility in men with and without asthenospermia: preliminary results. *Arch. Ital. di Urol. e Androl.* **87,** 14 (2015).

48. Corral-Baqués, M. I., Rivera, M. M., Rigau, T., Rodríguez-Gil, J. E., and Rigau, J. The effect of low-level laser irradiation on dog spermatozoa motility is dependent on laser output power. *Lasers Med. Sci.* **24,** 703–713 (2009).

49. Peterson, E. P., Moghissi, K. S., Paulsen, C. A., and Lipshultz, L. I. New guidelines for the use of semen donor insemination: 1986. *Fertil. Steril.* **46,** S95–S99 (1986).

50. DiMarzo, S. J., Huang, J., Kennedy, J. F., Villanueva, B., Hebert, S. A., and Young, P. E. Pregnancy rates with fresh versus computer-controlled cryopreserved semen for artificial insemination by donor in a private practice setting. *Am. J. Obstet. Gynecol.* **162,** 1483–1490 (1990).

51. Huang, Y.-Y., Sharma, S. K., Carroll, J., and Hamblin, M. R. Biphasic dose response in low level light therapy - an update. *Dose-Response* **9,** 602–18 (2011).

52. Kim, H. S. H. H. S., Kang, M. J., Kim, S. H. S. A., Oh, S. K., Kim, H. S. H. H. S., Ku, S. Y., Kim, S. H. S. A., Moon, S. Y., and Choi, Y. M. The utility of sperm DNA damage assay using toluidine blue and aniline blue staining in routine semen analysis. *Clin. Exp. Reprod. Med.* **40,** 23–28 (2013).

53. Fernandez, J. L., Muriel, L., Rivero, M. T., Goyanes, V., Vazquez, R., and Alvarez, J. G. The Sperm Chromatin Dispersion Test: A Simple Method for the Determination of Sperm DNA Fragmentation. *J. Androl.* **24,** 59–66 (2003).

54. Evenson, D. P., Jost, L. K., Larson, K. L., and Jost, L. K. Sperm Chromatin Structure Assay : Its Clinical Use for Detecting Sperm DNA Fragmentation in Male Infertility and Comparisons With Other Techniques Andrology Lab Corner. *J. Androl.* **23,** 25–43 (2002).

55. König, K., Liang, H., Berns, M. W., and Tromberg, B. J. Cell damage in near-infrared multimode optical traps as a result of multiphoton absorption. *Opt. Lett.* **21,** 1090–1092 (1996).

56. Singer, R., Sagiv, M., Barnet, M., Levinsky, H., Segenreich, E., Fuchs, Y., Mendes, E., and Yehoshua, H. Low energy narrow band non-coherent infrered illumination of human semen and isolated sperm. *Andrologia* **23,** 181–184 (1991).

57. Zan-Bar, T., Bartoov, B., Segal, R., Yehuda, R., Lavi, R., Lubart, R., and Avtalion, R. R. Influence of visible light and ultraviolet irradiation on motility and fertility of mammalian and fish sperm. *Photomed. Laser Surg.* **23,** 549–555 (2005).

58. Abdel-Salam, Z., Dessouki, S. H. M., Abdel-Salam, S. A. M., Ibrahim, M. A. M.,

and Harith, M. A. Green laser irradiation effects on buffalo semen. *Theriogenology* **75,** 988–994 (2011).

59. Lubart, R., Friedmann, H., Levinshal, T., Lavie, R., and Breitbart, H. Effect of light on calcium transport in bull sperm cells. *J. Photochem. Photobiol. B Biol.* **15,** 337–341 (1992).

60. Vesich, T. L. and Kramar, M. I. Study of the action of laser irradiation on the native and cryopreserved human spermatozoa. *Probl. Cryobiol.* **2,** 53–54 (1994).

61. Ban Frangez, H., Frangez, I., Verdenik, I., Jansa, V., and Virant Klun, I. Photobiomodulation with light-emitting diodes improves sperm motility in men with asthenozoospermia. *Lasers Med. Sci.* **30,** 235–240 (2014).

62. Sato, H., Landthaler, M., Haina, D., and Schill, W. B. B. The Effects of Laser Light on Sperm Motility and Velocity in vitro. *Andrologia* **16,** 23–25 (1984).

63. Corral-Baqués, M. I., Rigau, T., Rivera, M., Rodríguez, J. E., and Rigau, J. Effect of 655-nm diode laser on dog sperm motility. *Lasers Med. Sci.* **20,** 28–34 (2005).

64. Lenzi, A., Claroni, F., Gandini, L., Lombardo, F., Barbieri, C., Lino, A., and Dondero, F. Laser radiation and motility patterns of human sperm. *Arch. Androl.* **23,** 229–234 (1989).

65. Andrabi, S. M. H. and Maxwell, W. M. C. A review on reproductive biotechnologies for conservation of endangered mammalian species. *Anim. Reprod. Sci.* **99,** 223–243 (2007).

66. Nagashima, J. B., Sylvester, S. R., Nelson, J. L., Cheong, S. H., Mukai, C., Lambo, C., Flanders, J. A., Meyers-Wallen, V. N., Songsasen, N., and Travis, A. J. Live births from domestic dog (Canis familiaris) embryos produced by in vitro fertilization. *PLoS One* **10,** 1–13 (2015).

67. Durrant, B. S. The importance and potential of artificial insemination in CANDES (companion animals, non-domestic, endangered species). *Theriogenology* **71,** 113–122 (2009).

68. Hyun, N., Chandsawangbhuwana, C., Zhu, Q., Shi, L. Z., Yang-Wong, C., and Berns, M. W. Effects of viscosity on sperm motility studied with optical tweezers. *J. Biomed. Opt.* **17,** 25005 (2012).

69. O'Connell, M., McClure, N., and Lewis, S. E. M. The effects of cryopreservation on sperm morphology, motility and mitochondrial function. *Hum. Reprod.* **17,** 704–709 (2002).

70. Donnelly, E. T., McClure, N., and Lewis, S. E. M. Cryopreservation of human semen and prepared sperm: Effects on motility parameters and DNA integrity.

Fertil. Steril. **76,** 892–900 (2001).

71. Lasley, B. L., Loskutoff, N. M., and Anderson, G. B. The limitation of conventional breeding programs and the need and promise of assisted reproduction in nondomestic species. *Theriogenology* **41,** 119–132 (1994).

72. Preece, D., Chow, K. W., Gomez-Godinez, V., Gustafson, K., Esener, S., Ravida, N., Durrant, B., and Berns, M. W. Red light improves spermatozoa motility and does not induce oxidative DNA damage. *Sci. Rep.* **7,** 46480 (2017).

73. Nascimento, J. M., Shi, L. Z., Meyers, S., Gagneux, P., Loskutoff, N. M., Botvinick, E. L., and Berns, M. W. The use of optical tweezers to study sperm competition and motility in primates. *J. R. Soc. Interface* **5,** 297–302 (2008).

74. Chen, C.-S., Chao, H.-T., Leng, C.-H., Pan, R.-L., and Wei, Y.-H. Direct measurement of the tail beat frequency of human sperm by flashlight synchronization. *Andrologia* **54,** 49–54 (1998).

75. Patrizio, P., Liu, Y., Sonek, G. J., Berns, M. W., and Tadir, Y. Effect of pentoxifylline on the intrinsic swimming forces of human sperm assessed by optical tweezers. *J. Androl.* **21,** 753–756 (2000).

76. Westphal, L. M., el Dansasouri, I., Shimizu, S., Tadir, Y., and Berns, M. W. Exposure of human spermatozoa to the cumulus oophorus results in increased relative force as measured by a 760 nm laser optical trap. *Hum. Reprod.* **8,** 1083–1086 (1993).

77. Baba, T., Azuma, S., Kashiwabara, S. I., and Toyoda, Y. Sperm from mice carrying a targeted mutation of the acrosin gene can penetrate the oocyte zona pellucida and effect fertilization. *J. Biol. Chem.* **269,** 31845–31849 (1994).

78. Lopez, L. C. and Shur, B. D. Redistribution of mouse sperm surface galactosyltransferase after the acrosome reaction. *J. Cell Biol.* **105,** 1663–1670 (1987).

79. Baltz, J. M., Katz, D. F., and Cone, R. a. Mechanics of sperm-egg interaction at the zona pellucida. *Biophys. J.* **54,** 643–654 (1988).

80. Araujo, E., Tadir, Y., Patrizio, P., Ord, T., Silber, S., Berns, M. W., and Asch, R. H. Relative force of human epididymal sperm. *Fertil. Steril.* **62,** 585–590 (1994).

81. Tadir, Y., Wright, W. H., Vafa, O., Ord, T., Asch, R. H., and Berns, M. W. Force generated by human sperm correlated to velocity and determined using a laser generated optical trap. *Fertil. Steril.* **53,** 944–7 (1990).

82. Castellini, C., Dal Bosco, A., Ruggeri, S., and Collodel, G. What is the best frame rate for evaluation of sperm motility in different species by computer-assisted

sperm analysis? *Fertil. Steril.* **96,** 24–27 (2011).

83. Preece, D., Bowman, R., Linnenberger, A., Gibson, G., Serati, S., and Padgett, M. Increasing trap stiffness with position clamping in holographic optical tweezers. *Opt. Express* **17,** 22718–22725 (2009).

84. Bui, A. A. M., Stilgoe, A. B., Nieminen, T. A., and Rubinsztein-Dunlop, H. Calibration of nonspherical particles in optical tweezers using only position measurement. *Opt. Lett.* **38,** 1244–6 (2013).

85. Mcalinden, N., Glass, D. G., Millington, O. R., Wright, A. J., Wei, 4 X, Si, M., Imagawa, D. K., Ji, P., Tromberg, B. J., and Cahalan, M. D. Accurate position tracking of optically trapped live cells. *Biomed. Opt. Express* **5,** 1026–1037 (2014).

86. Subramani, E., Basu, H., Thangaraju, S., Dandekar, S., Mathur, D., and Chaudhury, K. Rotational dynamics of optically trapped human spermatozoa. *ScientificWorldJournal.* **2014,** 154367 (2014).

87. Tadir, Y., Wright, W. H., Vafa, O., Ord, T., Asch, R. H., and Berns, M. W. Micromanipulation of sperm by a laser generated optical trap. *Fertil. Steril.* **52,** 870–3 (1989).

88. Nascimento, J. M., Botvinick, E. L., Shi, L. Z., Durrant, B., and Berns, M. W. Analysis of sperm motility using optical tweezers. *J. Biomed. Opt.* **11,** 44001 (2006).

89. Piomboni, P., Focarelli, R., Stendardi, A., Ferramosca, A., and Zara, V. The role of mitochondria in energy production for human sperm motility. *Int. J. Androl.* **35,** 109–124 (2012).

90. Lyons, G., Bilgeri, A., Zanzinger, M., Berzin, M., and Mendelsohn, D. Extraction and estimation of ATP from human spermatozoa. *Andrologia* **18,** 455–460 (1986).